5-2017

Physical Characterization of Electrodeposited PCB Copper Foil Surfaces

Blessing Kolawole Ojo
University of South Carolina

PHYSICAL CHARACTERIZATION OF ELECTRODEPOSITED PCB COPPER FOIL SURFACES

by

Blessing Kolawole Ojo

Bachelor of Engineering
Covenant University, 2012

Submitted in Partial Fulfillment of the Requirements

For the Degree of Master of Science in

Electrical Engineering

College of Engineering and Computing

University of South Carolina

2017

Accepted by:

Paul G. Huray, Director of Thesis

Yinchao Chen, Reader

Guoan Wang, Reader

Cheryl L. Addy, Vice Provost and Dean of the Graduate School

DEDICATION

I dedicate this thesis to my mother and my family whose support made this work possible. I will always appreciate and be forever grateful.

ACKNOWLEDGEMENTS

I will like to acknowledge, first of all, my amiable and erudite Professor, advisor and committee chair Dr. Paul G. Huray. His dedication and understanding of electromagnetism has really caused notable breakthroughs and also impacted a wealth of knowledge into me. He was indeed more like a father, mentor, friend and at the same time a great teacher. Dr. Huray's Integral research and development of the Huray surface roughness model and guidance also added enormous information to the success of this thesis.

A special thanks also to Michael Griesi who made a duty to explain in details several issues I encountered and whose work I used as a foundation for this thesis. The feedback and responses were indeed impactful, helpful, insightful and constructive.

I would also like to thank John Fatcheric and Lee Lesher of Oak-Mitsui for their help, time contribution to getting required measurements, providing of the materials needed, and also provided required explanation to help through the research process. Without John and Lee's willingness to provide help, provide resources and impact their ideas and knowledge, it would not have been a success. Thank you all

ABSTRACT

Given that data rates of computers is on the rise and optimization of bus speeds continue to be of importance in improving the system performance, different models for a prediction of the impact of the surface roughness of copper foil have been developed and incorporated into different software's and applications used by design engineers.

With different models known to have been created for characterization of electrodeposited copper, they have been mostly affected by the need for higher frequencies as they are mostly useful for prediction at frequency of a few GHz. With the introduction of a new model (known as Huray Model which has helped with the prediction of losses of up to 50GHz and well improving towards 100GHz) which involves including surface features of electrodeposited copper foil and also making use of workable assumptions for estimating signal power loss. This model has been widely incorporated by several organizations into electromagnetic field simulators used commercially in industries today.

With all this said, it is still difficult to obtain accurately some of the parameters needed in estimation of the conductor losses which involves establishing a more standard approach of characterizing the electrodeposited copper foil in directly implementing the Huray Model for use in high speed circuit.

The main purpose of this thesis is therefore to obtain accurately these parameters, compare how the parameters differ on different copper foils, estimate the surface power loss of each copper foils compared, estimate the impact of volume on this losses and include dipole parameters in the Huray model over a higher frequency range (say 100THz).

This thesis is set to explain improved ways of obtaining parameters used in the "snowball" model for characterization of electrodeposited copper foil and performance of different copper foils using the snowball model. It also estimates the impact of absorbed and scattered parameters in surface power loss and also reveals some irregularities, difficulties and future recommendations.

PREFACE

The purpose of this thesis is to demonstrate the impact of surface roughness features on surface power loss of a copper foil considering the effect of dipole terms, absorption and scattering cross-section and also introduce a new technique on the characterization of copper foil nodules.

There are six (6) chapters in this research. Chapter one (1) involves the rationale behind this research. Chapter two(2) explains further review on the background for electro-deposited copper foil and Huray Surface Roughness Model. Chapter three (3) discusses the main objective of this research by demonstrating techniques involved in the characterization of the surface of electrodeposited copper foil and the impact of absorption and scattering cross-sections in Surface Power Loss with notable results. Chapter four (4) demonstrates the impact of dipole terms, absorption and scattering cross-sections on surface power loss by considering different copper foil types manufactured by Oak-Mitsui.

Chapter five (5) draws out conclusions based on obtained results, and also explains issues and concerns in obtaining accurate results in characterization of electro-deposited copper foil. Chapter six (6) explains the major contributions made to his thesis, important take-aways and future work recommendations.

TABLE OF CONTENTS

LIST OF TABLES

LIST OF FIGURES

LIST OF SYMBOLS

ρ	Material Resistivity (Ohm-Meter)
σ	Material Conductivity (Siemens per Meter)
Area	(Meter squared)
A_{matte}	Untreated surface area of the copper foil (Meter squared)
A_{flat}	Copper Foil flat surface area(Meter squared)
a_i	Radius of the snowballs (Copper Nodules) (Meters)
f	Frequency (Hertz)
H_0	Magnetic Field Intensity (Amperes per Meter)
η	Intrinsic Impedance (Ohms)
k_2	Wave Number (Meters)
l	Conductor Length (Meters)
μ_0	Permeability of Free Space (Henry per Meter)
δ	Skin Depth (Meter)
ε_0	Permittivity of Free Space (Farads per Meter)
$\varepsilon_{r,2}$	Relative Permittivity (Dimensionless)
N_i	Total Number of Snowball of radial size a_i (Dimensionless)
P_{loss}	Power Loss (Watts)
P_{rough}	Surface Power Loss of a Rough Conductor (Watts)
P_{smooth}	Surface Power Loss of a Smooth Conductor (Watts)

$R_{conductor}$	Resistance (Ohms)
$\sigma_{absorption}$	Absorption Cross Section of Radial Size ai (Meter Squared)
$\sigma_{scattered}$	Scattered Cross Section of Radial Size ai (Meter Squared)
σ_{total}	Total Absorption and Scattered Cross Section (Meter Squared)
ω	Angular Frequency (Radians per Second)

LIST OF ABBREVIATIONS

DC ..... Direct Current

ED ..... Electrodeposited

Hz ..... Hertz

MHz ..... Mega-Hertz

GHz ..... Giga-Hertz

THz ..... Tera-Hertz

MLS ..... Multi-layer Shiny side treatment

PCB ..... Printed Circuit Board

RGB ..... Red Green Blue

RMS ..... Root Mean Square

SEM ..... Scanning Electron Microscope

VNA ..... Vector Network Analyzer

TOB III ..... Treatment of Brass grade III

CHAPTER 1

INTRODUCTION

There has been several improvement to bus speeds over the years with frequencies edging towards 8GHz (16Gbps) and prospect of higher frequencies especially with the release of PCIe Generation 4 and other emerging technology such as PAM-4 technology. PCIe, especially continues to evolve from literally version 1.0 which was 2.5GT/s in 2002 to version 4.0 which is 16GT/s in 2016 which has made it important to consider the impact of signal power loss as these tends to impede the success of high speed circuit designs, interface protocols and technologies.

There is therefore the need to make estimable and accurate predictions of power loss associated with copper foils used in the manufacture of printed circuit boards which are used in high frequency circuit designs. Low frequency circuits could easily be designed and the power loss estimation conducted but the high frequencies design using the same model as that of low frequency has become difficult considering the surface roughness on "real-world" printed circuit board copper foil conductors which tend to cause a large deviation in actual power loss compared to a theoretical estimation.

This brought about the development of Huray surface roughness model which is an improvement over previous known models such as Morgan-Hammerstad and

Hemispherical models which has been used over the years for prediction of surface power loss and has therefore become inaccurate for higher frequency predictions.

Huray model, in which the first principles analysis of High frequency propagating EM field was used and Maxwell's field equations used in obtaining the losses, provides more accurate prediction for conductor loss with little or no deviation compared to the "real-world" surface power loss.

The Huray Model, also known as the "Snowball Model" has therefore, been incorporated in several EM field simulation softwares and also widely adopted in the industry and there has been need to further improve on how the parameters needed by the Huray model are obtained.

CHAPTER 2

BACKGROUND

2.1 HIGH SPEED TRANSMISSION LINES CONDUCTOR LOSSES

An estimation of conductor power loss has been effectively given by Joule's Law at DC and low frequencies:

$$P_{loss} = I^2 * R_{conductor} \quad (1)$$

Where P_{loss} is called the heat power loss in Watts (W), I is known as current flowing through the conductor in Amperes (A), and $R_{conductor}$ is the DC conductor resistance in Ohms (Ω).

$R_{conductor}$ is given as

$$\frac{\rho * l}{A} \quad (2)$$

Where ρ is the resistivity in Ωm, length (l) is the conductor length in meters and A is the cross-sectional conductor area in m^2. It is also known that increases in the conductor signal frequency leads to an effective reduction in the cross-sectional area of the conductor because the electric current density resides largely on the surface of the conductor. This effect describes what is known as skin effect. This skin effect is due to eddy currents which are induced by the changing magnetic fields due to time alternating currents. The exponentially decaying penetration depth , also known as the skin depth , is a measure of the depth at which the current density falls to 1/e of its value near the surface of the conductor.

The skin effect is calculated using the formula:

$$\delta(f) = \frac{1}{\sqrt{\pi f \mu_0 \mu_r \sigma)}} \quad (3)$$

Where $\delta(f)$ is the skin depth of current density in meters, f is the frequency of propagating signal in Hz, μ_o is the permeability of free space (given by 4π x 10^{-7}H/m) measured in (Henry/meter), μ_r is the relative permeability of the material, and the conductivity ,σ, is measured in siemens/meter. Distribution of an alternating electric current (AC) within a conductor in which the current density becomes large near the conductor surface and decreases with greater depths in the conductor causes skin effect. This understanding is important to predicting current distribution and power losses encountered in a practical PCB conductor which is often made of a rough copper surface adhering to a dielectric material like FR-4. Obtaining a correct prediction of this rough surface impact on conductor losses therefore is of importance because we know there is a non-uniform current density on the conductor surface which harmonically oscillates in time.

2.2 COPPER FOIL ELECTRODEPOSITION

Copper, being one of the most extensively used metals in industries due to its intrinsic properties is used in the formation of metallic films. It is obtained through a method known as electro-deposition. This section introduces conductor surfaces used in high-speed PCB design. There are also a large diversity of foils made with different surface roughness, by utilizing various gain structures and treatments. Electro-deposited copper foils can be produced as high, standard, low and very low profile. There are typically 3 phases used in industry in accomplishing the foil fabrication process: Dissolution and purification, Electro-deposition and then surface treatments. This is

illustrated in Figure 2.1. After the dissolution and purification of raw copper, both electro-deposition and surface treatments (divided into section 2 & 3) are of great importance in copper foil with known surface roughness character. The surface treatment generally helps to produce copper of better capabilities for manufacturing considerations.

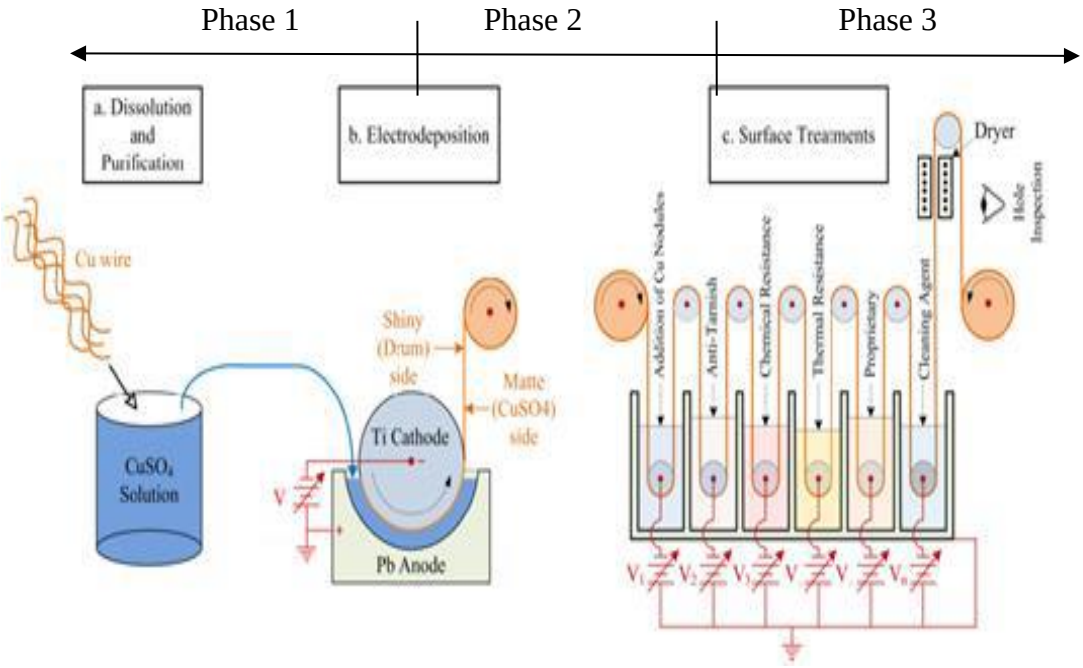

Figure 2.1: Electro-deposited copper foil fabrication

There are two sides of a copper foil; the drum and the matte side. These two sides are illustrated in figure 2.2 – 2.5 using the Oak-Mitsui samples for both the untreated and treated cases. There are also different copper foil profiles of varied importance. High profile copper is often used in low frequency applications which requires high bond strength between a copper trace and a board dielectric material like Fr-4 while low profile copper is often used to minimize signal conductor loss which deals with insertion losses intended for high frequency applications.

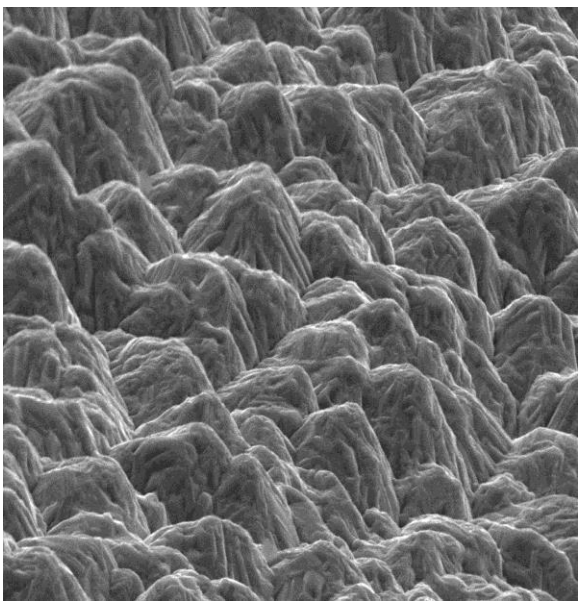

Figure 2.2 Oak-Mitsui untreated Copper foil
132750C TOB III 3500x (Matte)

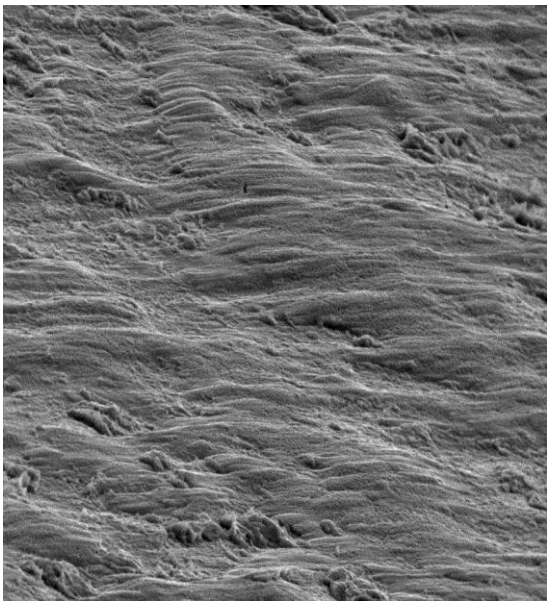

Figure 2.3 Oak-Mitsui untreated Copper foil
132772C MLS 3500x (Drum)

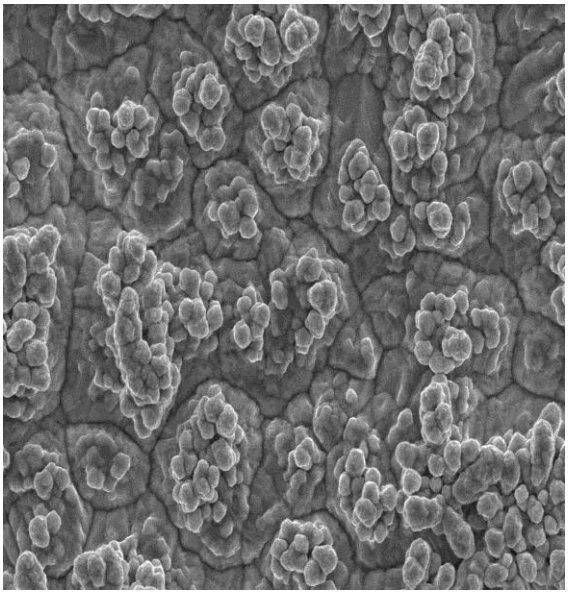

Figure 2.4 Oak-Mitsui Treated Copper foil
132750C TOB III 3500x (Matte)

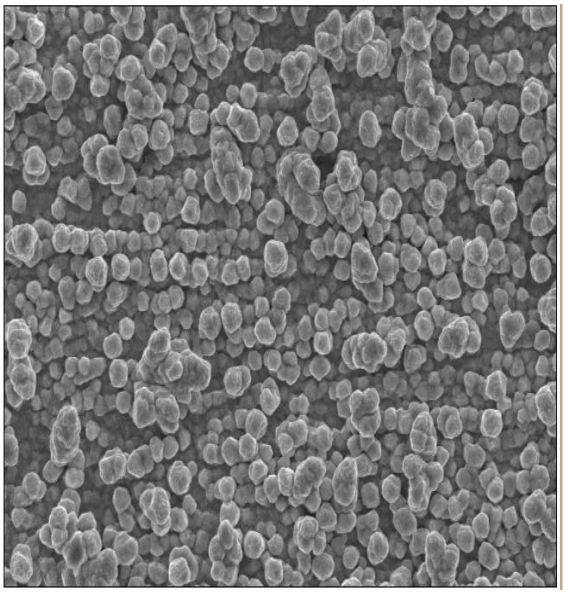

Figure 2.5 Oak-Mitsui Treated Copper foil
132772C MLS 3500x (Drum)

Figure 2.2 shows the untreated matte side of a type of Oak-Mitsui copper foil in which the purity, temperature, pH, buffering, and pressure of the $CuSO_4$ solution plays a key role in the surface roughness for this foil. Here the picture is of a high profile side of

electro-deposited copper foil. Figure 2.3shows the untreated drum side (shiny side) of the same type of copper foil from Oak-Mitsui in which surface roughness was mostly a result of the drum roughness or Ti (Titanium) cathode drum which is smoothened to ensure a flatter copper surface.

Subsequently, some treatments are performed on each of these untreated copper foils which basically changes their chemical resistance, thermal resistance, anti-tarnish character. An addition of copper nodules (or copper snowballs) helps with PCB adhesion to the adjacent dielectric material which is of great interest for PCB reliability and longer life. It is also been noted how manufacturers have a great deal of control on the distribution and size of the copper nodules deposited in which fabricated surface profile at the electro-deposition phase could have some effect on it. A scanning electron microscope image of treated (electrodeposited copper nodules on both the matte and the drum side) are illustrated in figure 2.4 & 2.5.

Having highlighted the basics of the copper foil production and how electro-deposition of copper foils are manufactured, we can now understand in-depth different models created to effectively estimate electrical signal surface power losses and their limitations.

2.3 HURAY DIPOLE SNOWBALL MODEL

To further understand more about this surface roughness and how it impacts the surface power-loss, Dr. Paul Huray using a first-principle analysis, described this conductor surface roughness power-loss with respect to the flat surface[The Foundations of Signal Integrity].

Neglecting the ($l=2$)quadrupole and higher ($l=3, \ldots$) multipole terms indicates that the ($l=1$) dipole terms produces (4).

$$\frac{P_{rough}}{P_{smooth}} \approx \left[\frac{\mu_0 \omega \delta}{4}|H_0|^2 A_{matte} + \sum_{i=1}^{j} N_i \sigma_{total,i} \frac{\eta}{2}|H_0|^2\right] / \left[\frac{\mu_0 \omega \delta}{4}\left||H_0|^2 A_{flat}\right.\right] \quad (4)$$

Where μ_0 is the permeability of free space in H/m, ω is the signal frequency component in a Fourier series in rad/s, H_0 is the local magnetic field intensity maximum in amperes/m , A_{matte} is the untreated copper foil surface area without the copper nodules in m^2, A_{flat} is the theoretically perfectly flat surface area of the copper foil in m^2, N_i is the total number of snowballs (copper nodules) per unit area, a_i is the radial size of each "snowball" (copper nodule), $\sigma_{total,I}$ is the total absorption and scattering cross sections of the copper nodules in m^2, and η is the intrinsic impedance of the propagating medium in ohms(Ω). Figure 2.5.5 shows the shape of these copper nodules which tend to be in a "snowball" shape. This led Dr Huray to approximate the snowball shapes as spheres; an approximation which is being used in equation (4).

Previous research work[Michael Griesi-Charaterization of electrodeposited copper foil] has used a more compact and approximate equation derived from the general equation (4) which tends to neglect the scattering parameters in its calculations. Using the dipole approximation (ignoring quadrupole and higher multipole terms) and the absorption terms (ignoring scattering terms) for perfect copper spheres, equation(4) reduces to (5)

$$\frac{P_{rough}}{P_{smooth}} \approx \frac{A_{matte}}{A_{flat}} + 6\sum_{i=1}^{j}\left[\frac{\frac{N_i \pi a_i^2}{A_{flat}}}{1+\frac{\delta}{a_i}+\frac{\delta^2}{a_i^2}}\right] \quad (5)$$

In this equation, neglecting the effect of the scattered power compared to absorbed power and also neglecting the quadrupole terms in the absorbed power is justified at lower frequencies; say below 100GHz for these foils. Below, we will show the error in neglecting the scattered power at higher frequencies (Say above 100GHz).

Giving that (5) helps with the surface power loss calculations while neglecting the scattering cross-section, (4) however gives a more complete overview and more accurate analysis for the surface power loss prediction by including both the absorption and scattering cross-section in its calculations.

The snowball approximation has demonstrated measurement correlation within an accuracy (in dB/in) within 1% for transmission line losses measured for frequencies of up to 50GHz for a 7'' microstrip. The snowball model is also capable of predicting transmission line power losses up to (and above) 100GHz.

Figure 2.6 shows a correlation between the theoretical results obtained from the snowball model and VNA measurements.

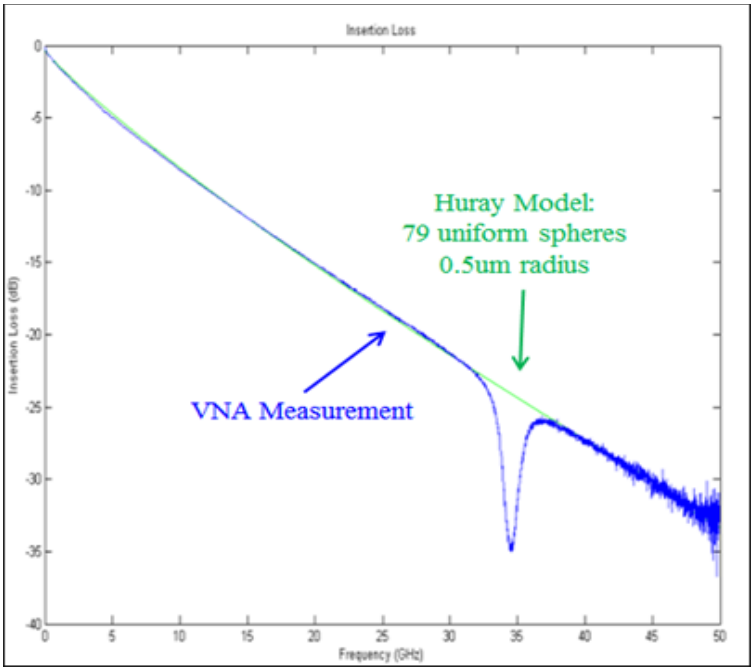

Figure 2.6 Snowball model as against VNA measurement

A propagating signal encountering a good conducting sphere causes the signal to either scatter or be absorbed and the total cross-section brings about sum of both absorbed and scattered properties.

In this case, dipole terms are only been considered which indicates that l = 1

Neglecting quadrupole and higher multipole terms and stating l=1, we obtain equations for dipole absorbed and scattered terms in (6) and (7).

$$\sigma_{absorbed}(\omega) \approx 3\pi k_2 a_i \delta/[1 + \frac{\delta}{a_i} + \frac{\delta^2}{a_i^2}] \quad (6)$$

and

$$\sigma_{scattered}(\omega) \approx \frac{10\pi}{3} k_2^4 a_i^6 [1 + \frac{2}{5}(\frac{\delta}{a_i})] \quad (7)$$

and

$$\sigma_{total} = \sigma_{absorbed} + \sigma_{scattered} \quad (8)$$

Where k_2 is the wave vector for non-conducting medium and giving as

$$k_2 = \omega\sqrt{\mu_0 \varepsilon_0 \varepsilon_{r,2}} \quad (9)$$

and Ƞ is the intrinsic impedance giving as

$$Ƞ = \sqrt{(\mu_0/\varepsilon_0 \varepsilon_{r,2})} \quad (10)$$

(7) and (8) respectively helps to calculate the absorbed and scattered power but (8) has been demonstrated to be negligible over a particular frequency and understanding when this scattered power becomes important is imperative. Figure 2.7 shows Absorption and scattering parameters of various sizes of copper spheres, that is, $a_i = 0.2um, 0.5um$ & $1um$ respectively and also supports the conclusion that scattered power could be negligible for frequencies up to 100GHz, and when the frequency exceeds that, the scattered power becomes significant.

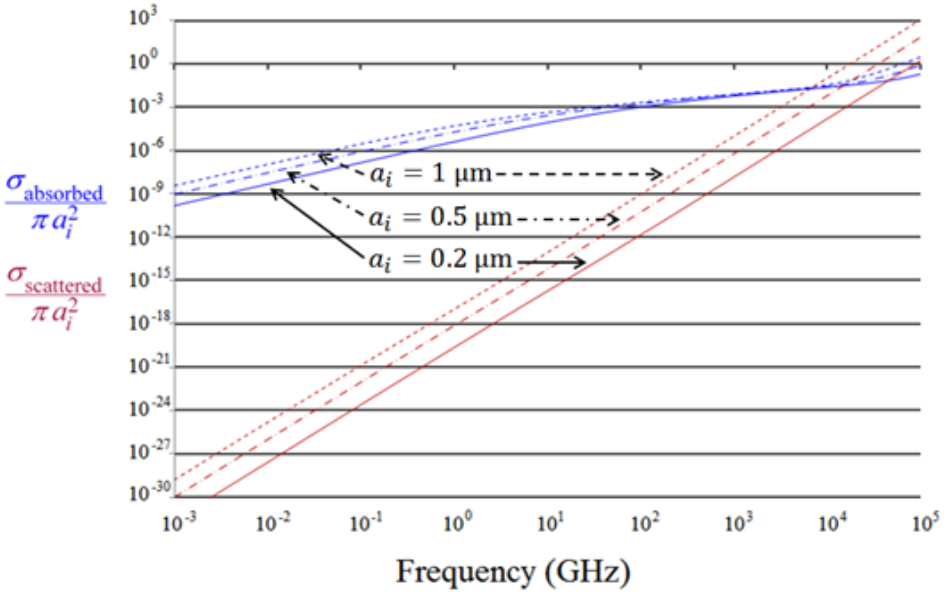

Figure 2.7 Absorption and Scattering cross-sections of 3 copper spheres

2.4 QUADRUPOLES

To further affirm the earlier assumption of neglecting quadrupole (l=2) and higher multipole terms, a plot of the quadrupole cross-section in figure 2.8 was obtained which shows the dipole terms are dominant and the quadrupole terms are indeed negligible.

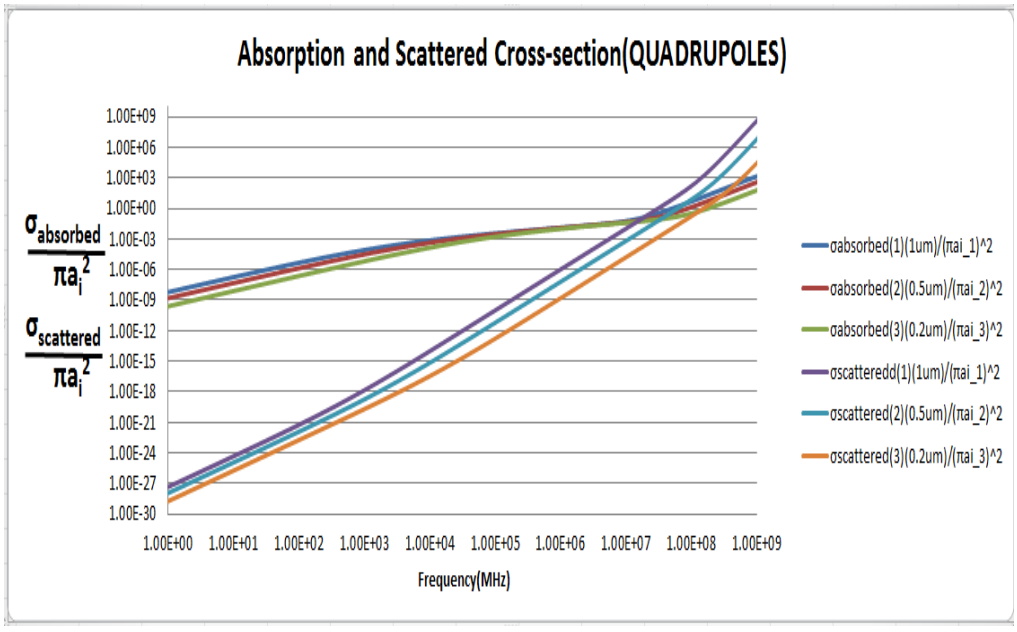

Figure 2.8 Absorption and scattering cross-section (Dipoles & Quadrupoles)

2.5 LIMITATIONS OF HURAY SNOWBALL MODEL

Even though the Huray model is easily implementable, an established method to characterize the copper foil surface to obtain parameters to implement the model has been a major issue. Some previous approximations are less accurate in obtaining these parameters.

Some assumptions were made which were known to overly simplify surface profile. First assumption involves averaging nodules snowball radii on a copper foil consisting of snowball radii distribution. Figure 2.9 illustrates this assumption

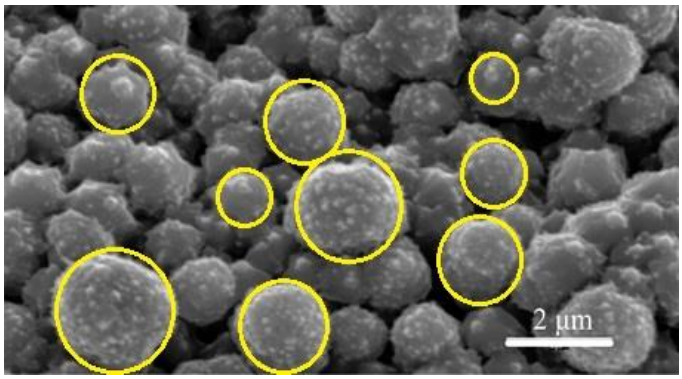

Figure 2.9 Different sizes of snowball

Second assumption involves Simplification of N_i/A_{flat} which assumes a flat raw copper foil and number of snowballs per unit flat area is being altered. Figure 2.10 illustrates this assumption

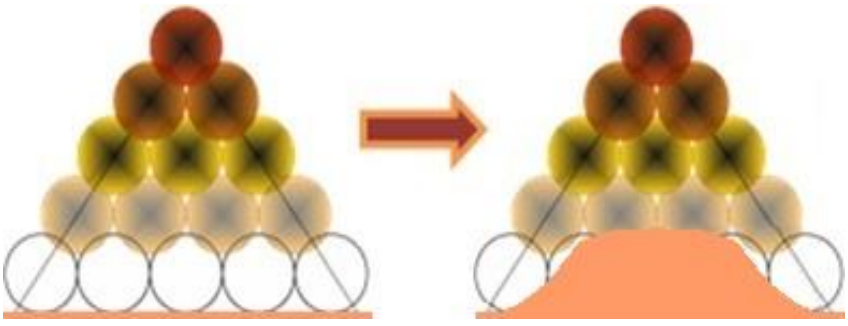

Figure 2.10 Flat raw copper foil with N_i(Left) & Irregular raw copper foil with N_i(Right)

It is also good to note that, different copper foils have different snowball densities, which means there are different number of snowballs per unit area.

2.6 SEM SUITABLE ANGLE OF CAPTURE

To further obtain more accurate result in characterizing the snowballs, a clear view of the SEMs are required to be effectively analyzed by the application to be used. This allowed for the SEMs to be taken at different angles and with 70^0 degree angle being the highest angle which the SEMs could be obtained using the 3D Microscope. Different angles of SEMs were obtained from 0 degree to 70 degrees which when processed, SEMs at 70degrees were clearer and have more precise results compared to the SEMs obtained at lower angles. Figure 2.12 – 2.15 illustrates the difference as seen from 0degree and 70 degrees.

MATTE SIDE

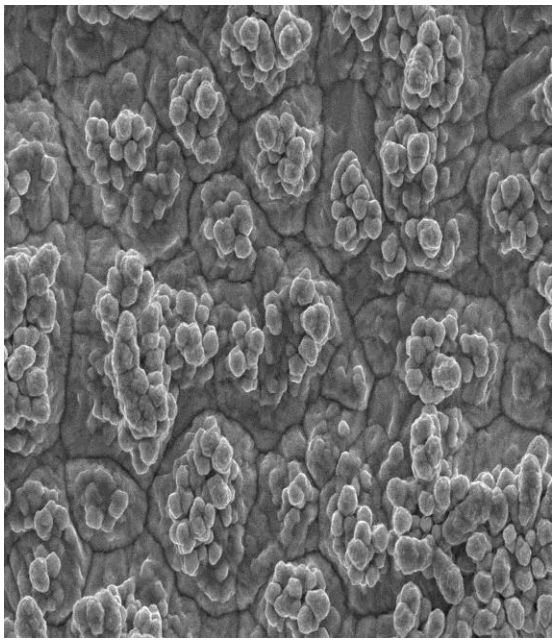

Fig. 2.11 Oak-Mitsui 132750C TOB III (0 Degree)3500x

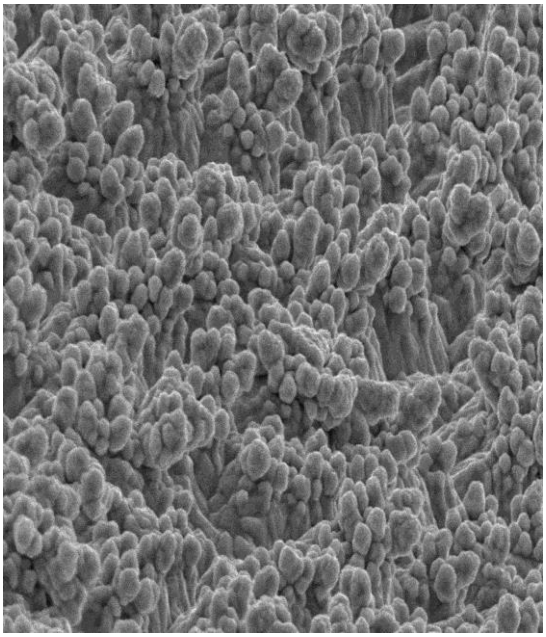

Fig. 2.12 Oak-Mitsui 132750C TOB III (70 degrees) 3500x

DRUM SIDE

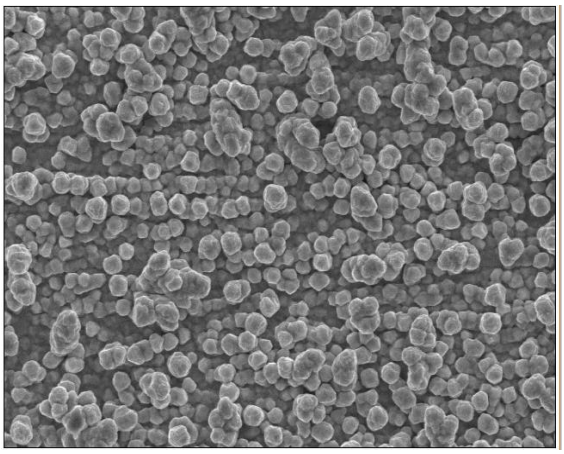

Fig. 2.13 Oak-Mitsui 132772C MLS (0 Degree)3500x

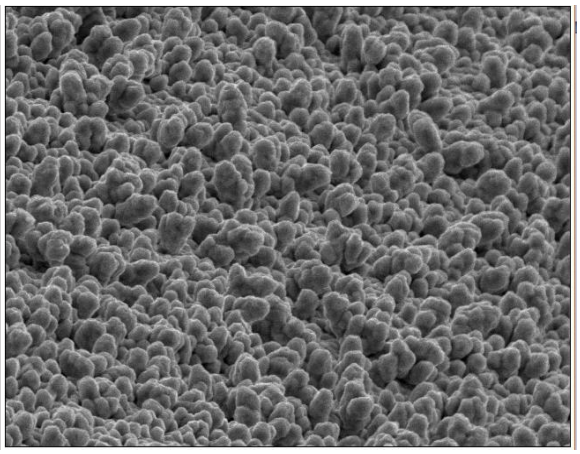

Fig. 2.14 Oak-Mitsui 132772C MLS (70 degrees) 3500x

CHAPTER 3

DIPOLE SURFACE POWER LOSS

3.1 EFFECT OF SNOWBALL MODEL PARAMETERS (INCLUDING DIPOLES) ON CONDUCTOR LOSS

In other to characterize copper foil and derive parameters to be used for the snowball model, it is essential to know that snowball radii distribution is necessary and it is essential to also understand what method of snowball radii distribution is best used for accurate analysis which includes either "Uniform snowball radii sizes" or "Snowball radii distribution". While the uniform snowball radii sizes involve identifying specific radial sizes of each snowballs, Snowball radii distribution involves creating a bin of several snowball sizes. This calculation was carried out mainly using "Uniform snowball radii sizes" but a comparison was assessed using different number of snowball sizes. The same total number of snowballs per unit flat area was also used in the assessment of the calculations. The first set of calculations were based on assumption of snowball sizes and also the total number of snowballs and a comparison was carried out between eight(8) snowball sizes(Figure 3.1) with (Figure 3.2 & 3.3) showing the absorption and scattering effect) and fifteen snowball sizes. Figure 3.4 to produce a wider range of snowball radial sizes. The results were as expected, as the higher the radial snowball sizes, the more accurate prediction for the surface power losses as compared with actual measured radial sizes recognizing that, actual copper foils have different radial size distribution. Snowball radii distribution would also make a great difference, as this would group

snowballs of different radial sizes and would contain almost all snowball radial sizes and produce a more realistic prediction.

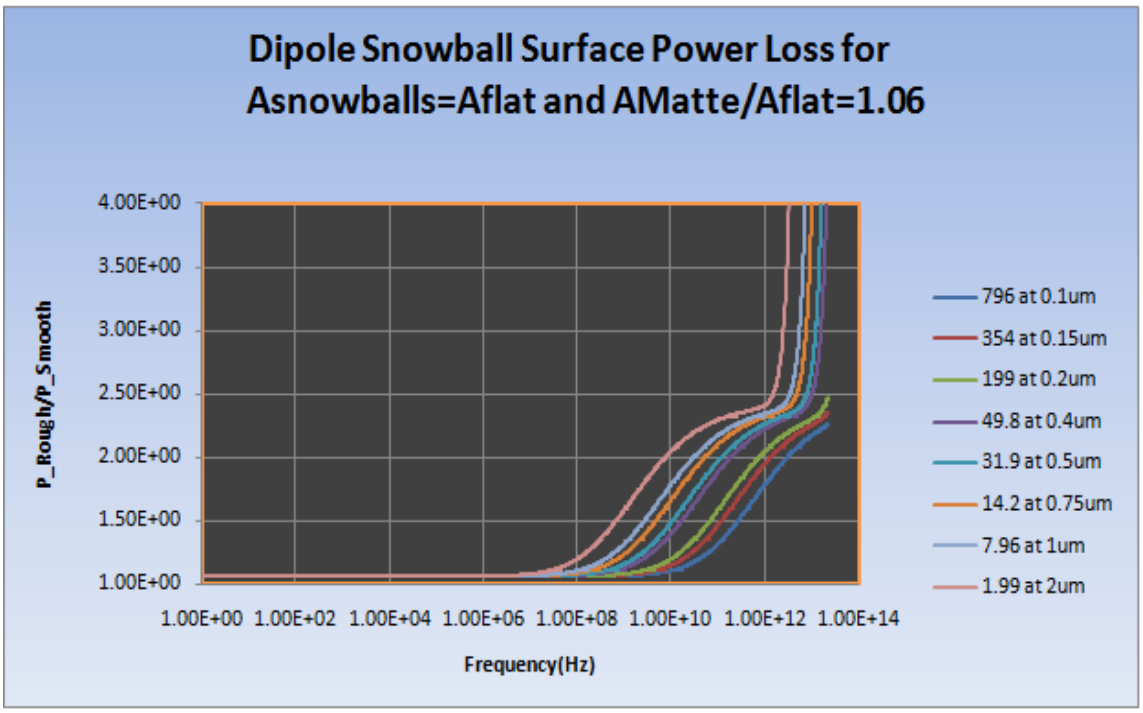

Figure 3.1 Distribution effect for 8 copper snowball sizes on surface power loss

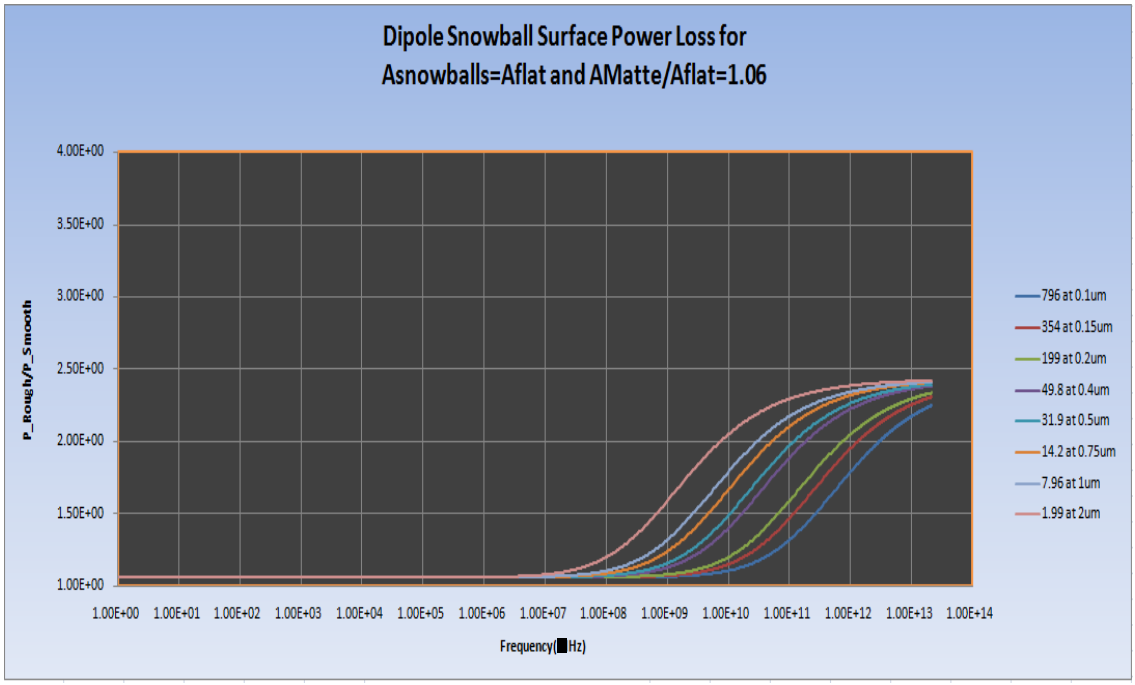

Figure 3.2 Dipole snowball surface power loss due to absorption

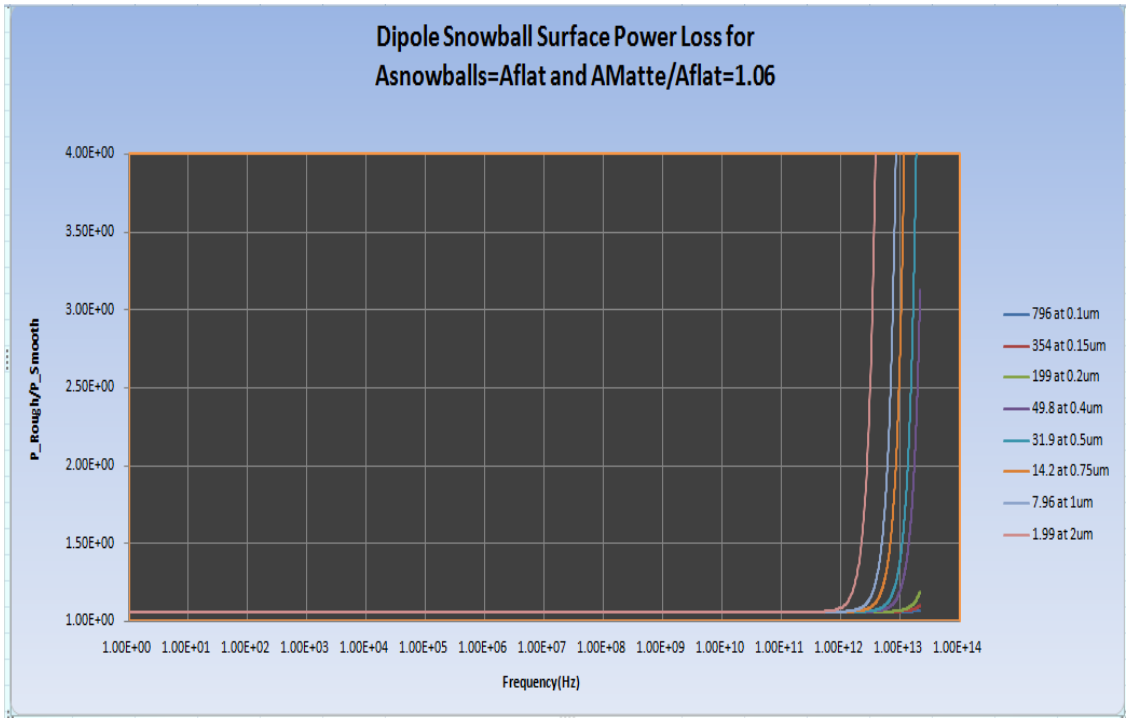

Figure 3.3 Dipole snowball surface powerloss due to scattering

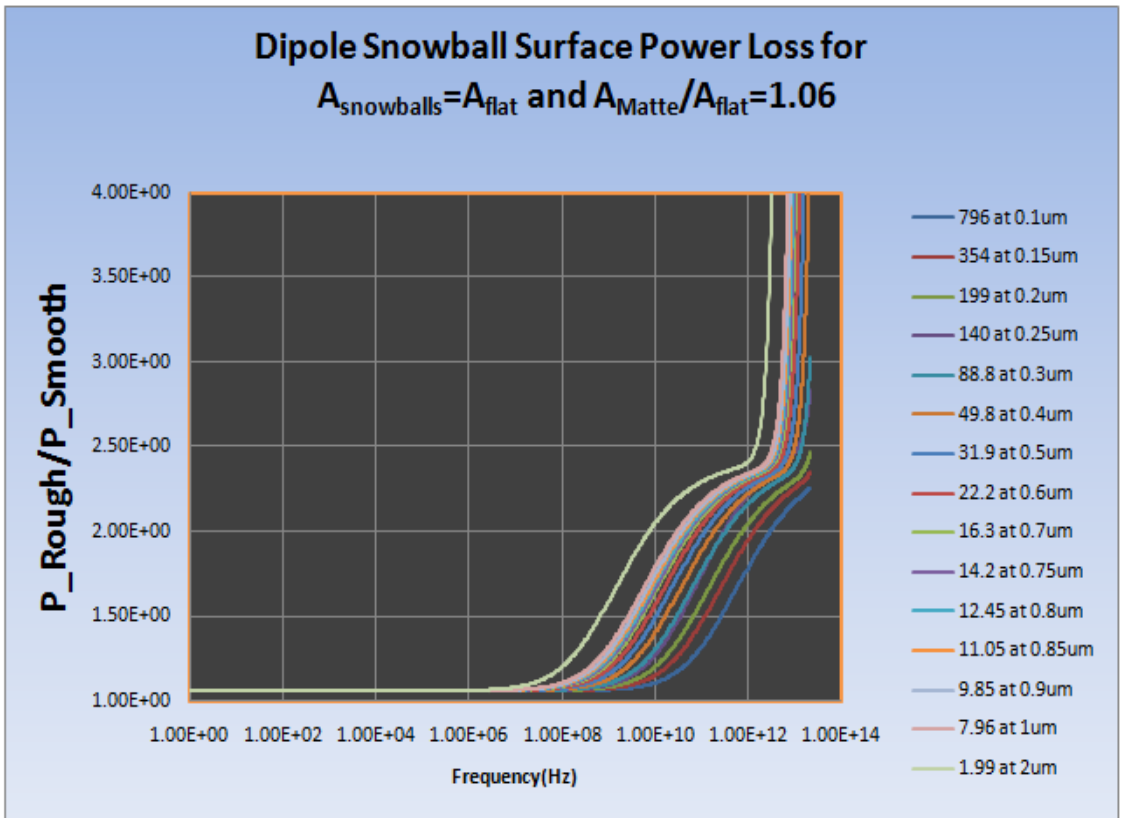

Figure 3.4 Distribution effect for 15 copper snowball sizes on surface power loss

3.2 TREATED COPPER FOIL: CHARACTERIZING SNOWBALL SIZES

Clear enough images of the treated copper surfaces are required to obtain (a_i)radial sizes distribution and also N_i/A_{flat} of the snowballs. A magnification of 3500x was used for this research. The method used was basically based on the images taken by the SEM. It was also noted that the angle at which each images were taken matters, in other to produce clearer images which makes it easier for the detection of the snowballs by necessary software/application being used.

Five (4) challenges were encountered in obtaining the required parameters (a_i and N_i/A_{flat}) and analysis:

1. Accurate identification of each snowballs
2. Accurate Identification of snowballs in layers
3. Accurate total count of the snowballs in the image
4. Measure the radius of each snowballs

Manually performing this 4 challenges will be a daunting task as it would be prone to errors and several inaccurate results. There are known approaches for automatic image detection such as binarization, which involves filtered background, but snowballs can be inadvertently clumped together thereby making it difficult to identify each snowballs accurately. Circular Hough Transform(CHT) was also preferred in other situation but it does not detect snowballs which exists in layers and lower precision in the total count of snowballs. Alternative angles could obtain higher clarity 2D images. Image thresholding, filtering, and watershed process which segments each snowball and analyze the image which gives a more accurate total count of the snowballs was used. A drawback to this approach would be to accurately identify all snowballs, especially snowballs in layers and

also the watershed process breaking bigger snowballs into smaller sizes.

3.2.1 SEM ANALYSIS METHOD

3.2.1.1 USING IMAGE J

The captured images of the both treated and untreated copper foil was carried out using the SEM called JSM-6360LV SEM. Figure 3.5 shows the SEM.

Figure 3.5 Scanning Electron Microscope (SEM)

Two magnifications were also compared (700x and 3500x) at an angle of 70degrees to certify the recommendation of magnification of either 700x or 3500x, of which both are still very much visible at the proposed angle, but 3500x provides the a larger field of view for the snowballs. 5 different samples of 4types of copper foils were analyzed from 4 different angles (0,20, 55 and 70 degrees). Figures 2.8-2.11(1 section for the treated drum side and 1 section for the treated matte side) illustrates captures of a copper foil at angles 0 and 70 degrees to illustrate the difference in clarity of the said 2D images.

After capturing the SEM images, an application known as Image J was used to effectively analyze the images and obtain the snowball radial size distribution and also

the total count for the number of snowballs (Figure 3.6). Image J is an application developed mainly for the detection of tiny red blood cells, which nearly accurate, filters the image, performs thresholding, uses watershed to segment each snowballs and gives the total count for the snowballs and also provides the distribution of the snowball sizes.

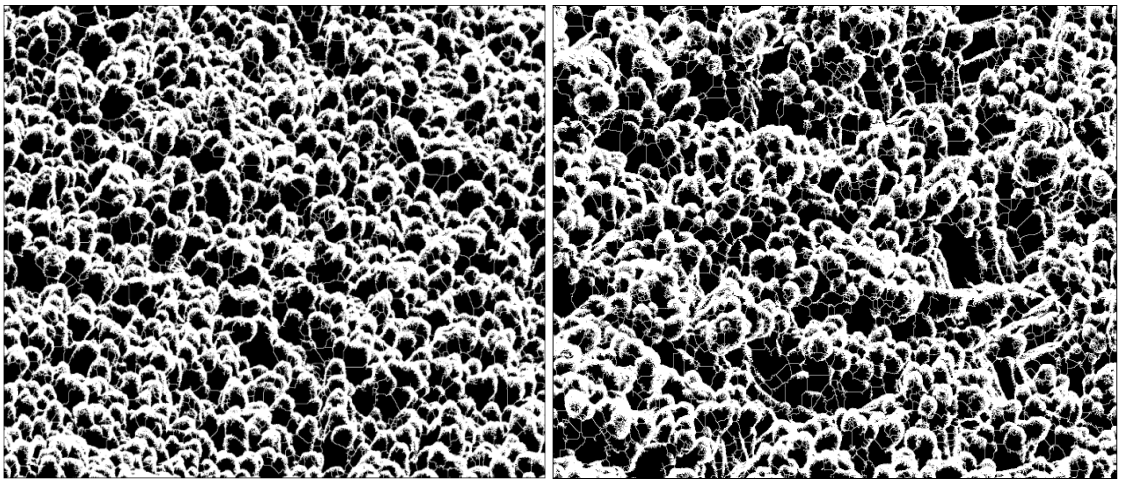

Figure 3.6 IMAGE J Snowballs on the Drum Side (Left) and the Matte Side (Right)

Although the analysis done by the Image J is dependent on the clarity of the 2D image used which basically increases the accuracy of the obtained results, it also requires fine tuning for effective analysis. Edge detection threshold could also be performed using the image J which provides information on whether too few or many snowballs is being identified. What actually differentiates Image J, which also uses binarization method from other normal binarization method is the watershed process.

Watershed process involves segmentation of each clumps of snowballs to make counting of snowballs effective but a drawback is about its sensitivity to breaking up larger snowballs into smaller ones which might increase the snowball count, and increase the count of smaller snowball sizes. Also, in Image J analysis, images needs its own settings to be done for effective analysis and also, even though it provides the distribution of snowballs, it does not accurately define the specific radial size for each characterized

snowball but creates bins for the snowballs. Figure 3.7 shows this snowball diameter distribution and also relevant information pertaining to the distribution.

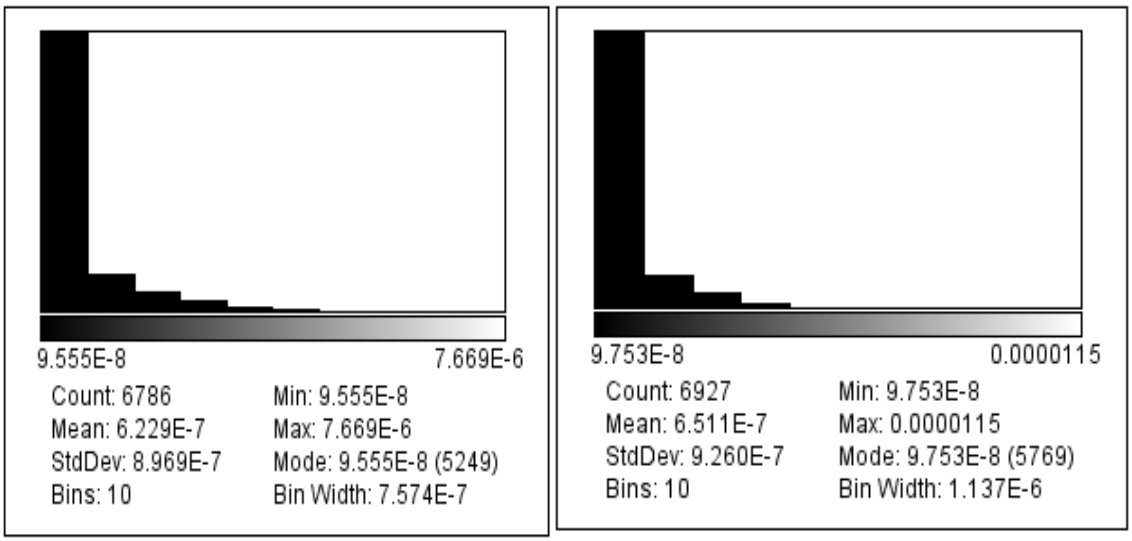

Figure 3.7 Diameter Distribution of Drum side (Left) and the Matte side (Right)from Image J

About 10 bins were generated for the distribution of snowballs. There was a set scale to effectively convert pixels to μm (about 1.45E6pixels/μm). This produced a result of an average a_i of 0.311μm, standard deviation of 0.48μm and an average N_i/A_{flat} of 104 snowballs per 100um^2 on the drum side with the smallest snowball size of approximately 0.05μm and the highest of 3.83μm. For the matte side, the result of an average a_i of 0.33μm and standard deviation of 0.46μm was generated with the smallest snowball size of approximately 0.05μm and highest of 5.75μm and an average N_i/A_{flat} of 106 snowballs per 100um^2. Also, given that the SEMs were taken at an angle of 70degrees, there would be a little reduction in the width considering the angle of capture factor. This 70^o was however, not considered in the Flat area calculation and assumed to be 1 which maintains the value of the width.

3.2.1.2 USING CHT (Circular Hough Transform)

This method was also used previously, and could also be an alternative choice because it could identify partially hidden snowballs as well as giving snowball counts and radial sizes but lower precision in the snowball count compared to the results obtained using image J. And it also works explicitly on 2D images. The method is been implemented using the MATLAB and it requires fine tuning to produce required result.

3.2.1.3 3D DIGITAL MICROSCOPE METHOD

The name of the Microscope used was KH-3900 3D Digital Microscope as seen in Figure 3.8.

Figure 3.8 Hirox KH-8700 3D DIGITAL MICROSCOPE

Not much emphasis was placed on this method due to several inaccuracies and difficulties it portrays. This microscope has software used to identify the snowballs and also produce radii distribution. It uses RGB thresholding and makes use of binarization to identify the snowballs. However, it rather clumps the snowballs in an area together, thereby making it difficult to isolate each snowball. This produces incorrect snowball count and sizes which makes the result unreliable.

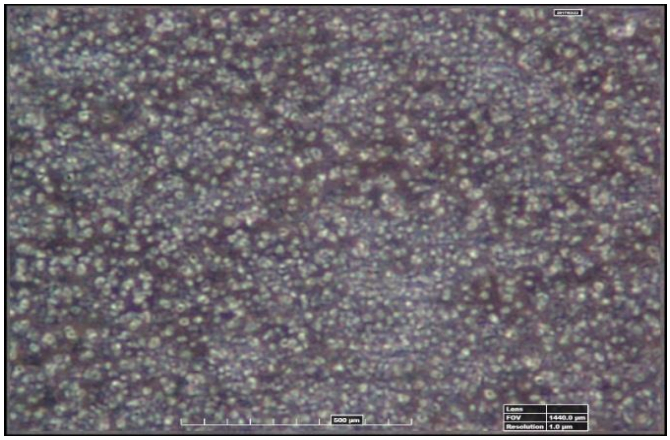

Figure 3.9 Obtained 3D Digital Microscope result

Unlike image J process, which is rather easy to use, it is time consuming to adjust different settings and parameters and isolate the snowballs and also difficult to obtain required results. Figure 3.9 above illustrates the result obtained by the microscope which lumps up several snowballs which was why less emphasis was placed on this method.

3.3 COMPARISON OF DIFFERENT COPPER FOILS

To further continue with this research, another approach was to select specific copper foils which were basically from Oak-Mitsui and compare different snowball distribution and the effect of this on losses.

Four (4) copper foils were selected each for both the drum and the matte side and analyzed. For the drum, they were : 132772C MLS,133069C MLS,133905C MLS and 132851C MLS and for the matte side, they were: 157017A TOB III, 179045B,157379A TOB III and 132750C TOB III.

3.3.1 DRUM SIDE

3.3.1.1 TYPE 132772C MLS

The snowball count on this copper foil is about 6786 copper snowballs as indicated in the result below. It has the lowest radial snowball size of approximately

0.05µm and highest snowball radial size of 3.8µm and an average N_i/A_{flat} of 104 snowballs per 100um^2.Obtained result is illustrated in Figure 3.10

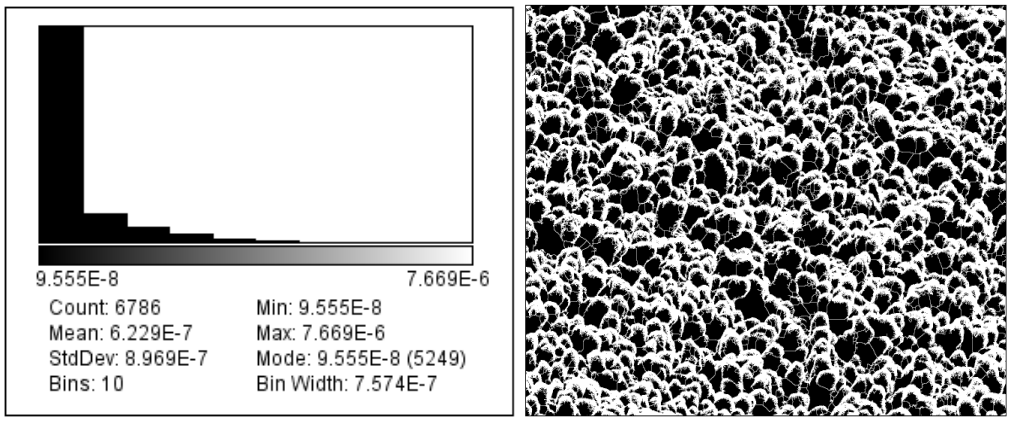

Figure 3.10 Diameter Distribution of Drum side (132772C MLS) from Image J (Distribution result on the left and copper snowball count on the right)

3.3.1.2 TYPE 133069C MLS

The snowball count on this type of copper foil was 6713 which was lower than the previous copper foil considered. It radial distribution ranged from approximately 0.05µm to 4.9µm and an average a_i snowball size of 0.326µm and an average N_i/A_{flat} of 103 snowballs per 100um^2. Obtained result is illustrated in Figure 3.11.

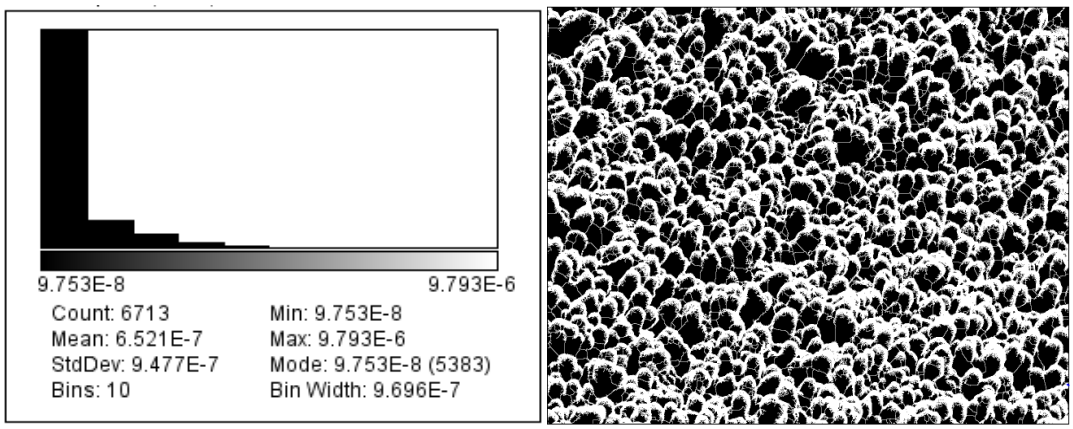

Figure 3.11 Diameter Distribution of Drum side (133069C MLS) from Image J (Distribution result on the left and copper snowball count on the right)

3.3.1.3 TYPE 132851C MLS

This type of copper foil compared to the previous two considered has the highest count of snowballs of 6819 with its radial distribution of the snowballs ranging from approximately 0.05µm and 3.5µm. It also has an average a_i snowball size of 0.32µm and an average of 104 snowballs per 100um^2. Obtained result is illustrated in Figure 3.12.

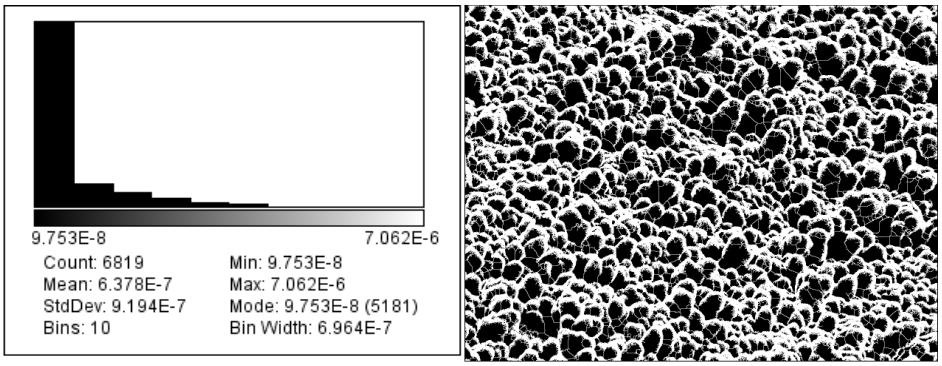

Figure 3.12 Diameter Distribution of Drum side (132851C MLS) from Image J (Distribution result on the left and copper snowball count on the right)

3.3.1.4 TYPE 133905C MLS

This type of copper foil compared to the previous three considered has the lowest count of snowballs of 2888 with its radial distribution of the snowballs ranging from approximately 0.05µm and 4.3µm. It also has an average a_i snowball size of 0.58µm and an average N_i/Aflat of 44 snowballs per 100um^2. Obtained result is illustrated in Figure 3.13

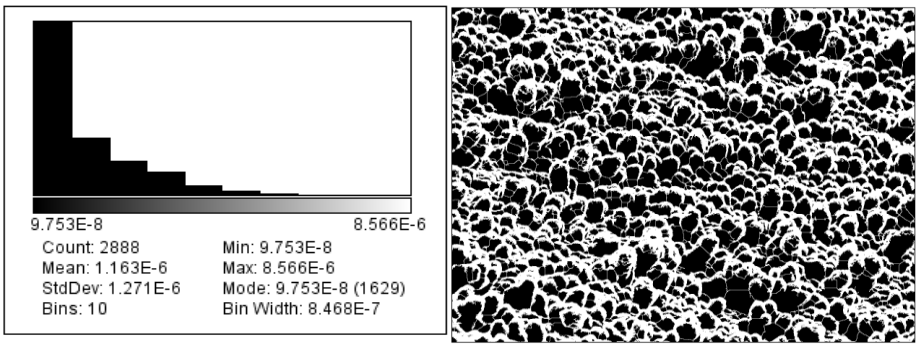

Figure 3.13 Diameter Distribution of Drum side (133905C MLS) from Image J (Distribution result on the left and copper snowball count on the right)

3.3.2 MATTE SIDE

3.3.2.1TYPE 132750C TOB III

The snowball count on this copper foil was 6927 which was the lowest compared to the other two copper foils examined in this category. The radial snowball size ranged from approximately 0.05µm to 5.75µm. It also has an average a_i snowball size of 0.325µm with a standard deviation of 0.463µm and an average N_i/A_{flat} of 106 snowballs per 100um^2. The result is shown in Figure 3.14.

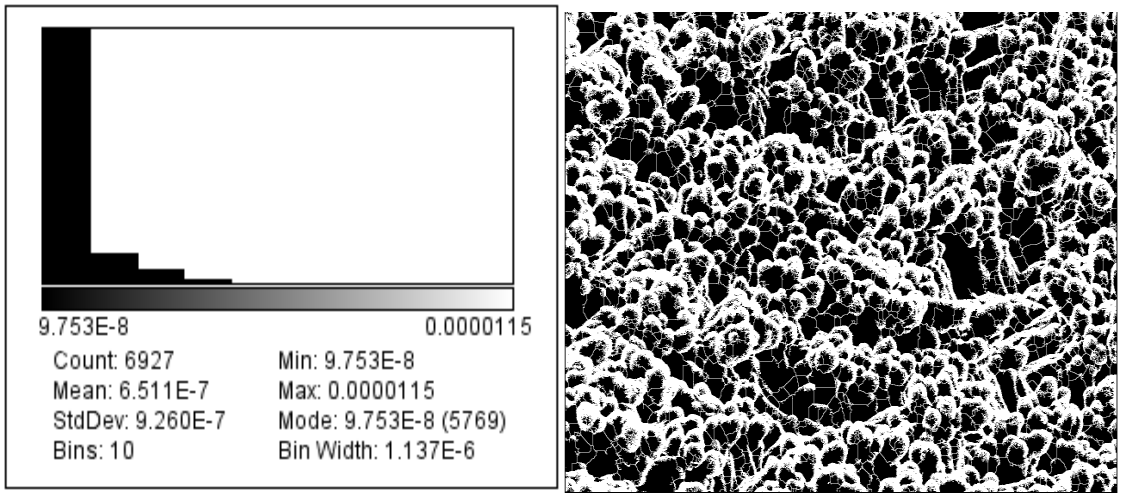

Figure 3.14 Diameter Distribution of Matte side (132750C TOB III) from Image J (Distribution result on the left and copper snowball count on the right)

3.3.2.2 TYPE 179045B TOB III

The snowball count on this copper foil was 7187 which was quite lower compared to the first one examined in this category. The radial snowball size ranged from approximately 0.05µm to 5.1µm. It also has an average a_i snowball size of 0.317µm with a standard deviation of 0.44µm and an average N_i/A_{flat} of 110 snowballs per 100um^2. The result is shown in Figure 3.15.

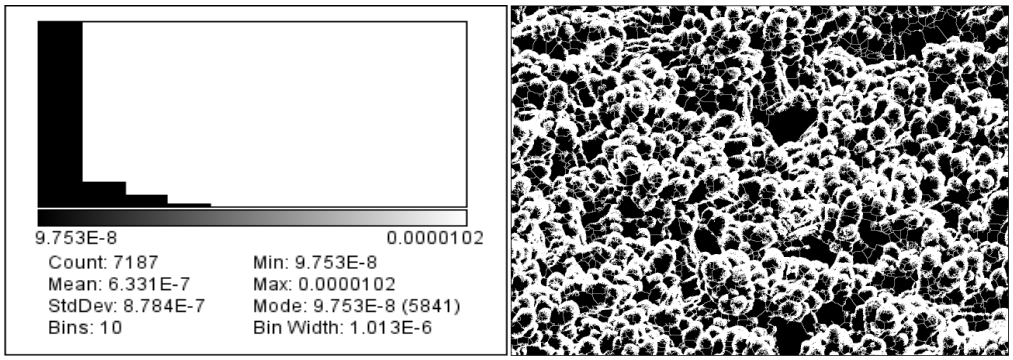

Figure 3.15 Diameter Distribution of Matte side (179045B TOB III) from Image J (Distribution result on the left and copper snowball count on the right)

With all copper foil types selected and analyzed, the effect of snowball counts and their respective radial sizes on losses would be analyzed which is expected to reveal which copper foil has a better performance and the losses quite minimal. Also in subsequent chapters, recommendations would be made on how this losses could be further reduced basically based on reduction of the snowballs.

3.3.1.3 TYPE 157017A TOB III

The snowball count on this copper foil was about 8055 using the same condition stated above for analysis. The radial snowball size ranged from 0.05μm to 4.4μm. It also has an average a_i snowball size of 0.288μm with a standard deviation of 0.42μm and an average of N_i/A_{flat} of 123 snowballs per $100um^2$. The result is shown in Figure 3.16.

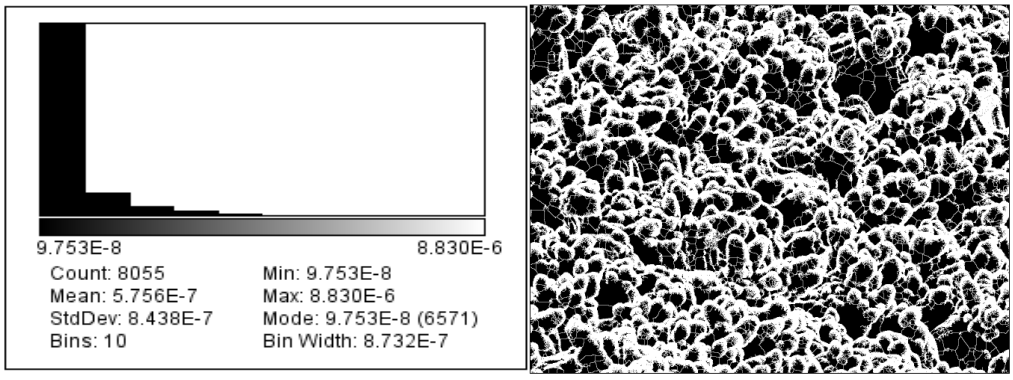

Figure 3.16 Diameter Distribution of Matte side (157017A TOB III) from Image J (Distribution result on the left and copper snowball count on the right)

3.3.1.4 TYPE 157379A TOB III

The snowball count on this copper foil was about 7339 using the same condition stated above for analysis. The radial snowball size ranged from 0.05μm to 3.77μm. It also has an average a_i snowball size of 0.308μm with a standard deviation of 0.43μm and an average N_i/A_{flat} of 112 snowballs per 100um^2. Obtained result is illustrated in Figure 3.17

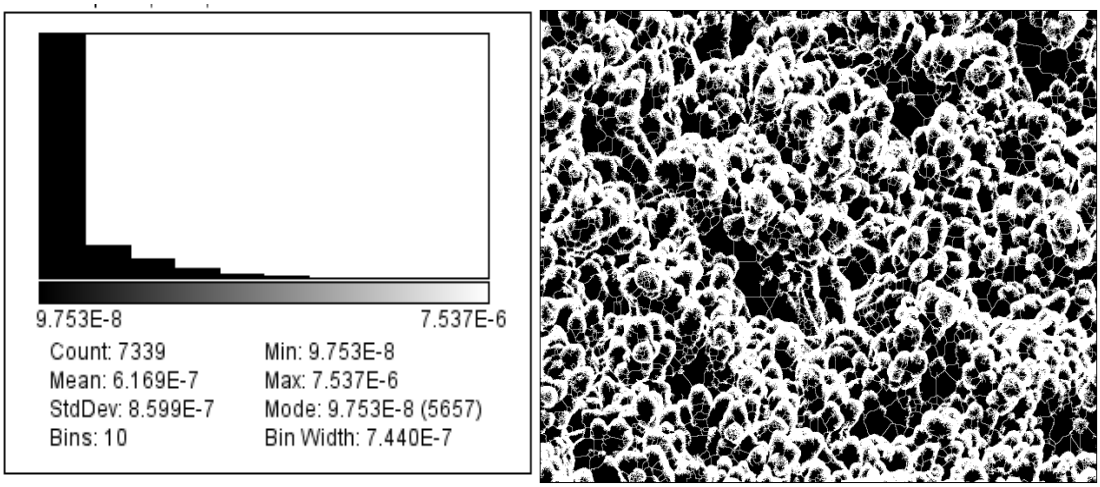

Figure 3.17 Diameter Distribution of Matte side (157379A TOB III) from Image J (Distribution result on the left and copper snowball count on the right)

3.4 SURFACE AREA CHARACTERIZATION OF UNTREATED COPPER FOIL (A_{matte}/A_{flat})

To obtain the surface area of the untreated copper foil, it is required to obtain the total length and width to include the peaks and valleys. Three methods are presented to achieve this and two of these three methods had been earlier proposed. The first method involves using the image J directly to obtain the surface area which could be automatically generated based on the in-built features but it might be difficult to ascertain if the area generated could be used for every copper foil which introduced some discrepancies in our results. Stack of images (in which image J allows just maximum of 2 images to be stacked) are introduced to obtain the area but the obtained area could not be

relied upon which will lead to each copper foil been measured individually which obviously results in different area obtained for each of the copper foil. Second method which was earlier proposed was using a mechanical profilometer (perthometer) which is widely used and it involves obtaining the length of the copper foil and the profilometer also provides information for other roughness parameters. Finally, the third method was using the 3D Digital microscope which also has in-built software to obtain the required area automatically and could allow the images to be stacked to properly obtain required area.

While the first and the third method could enable us obtain the area of the images automatically, the second method requires interpolation to obtain the right width and length of the proposed copper foil.

3.4.1 IMAGE J METHOD

The Image J version used to obtain the required area was Image J 1.50i shown in Figure 3.18.

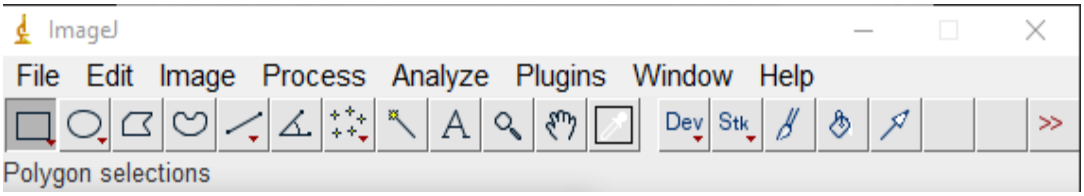

Figure 3.18 Image J Application

This simply involves importing the image, set the scale, because image J has its default scale set to pixels which needs to be converted to um, perform thresholding, which is the only way image J can analyze your image, and in this case, auto thresholding was performed as manual thresholding could be time consuming to obtain required image result and then select area as one of the required image output using the measurement

option on image J and then analyze the image. This tends to output both the minimum and maximum area and gives the average area for the entire imported image. Image J reports different area for each of the selected copper foils. Figure 3.19 shows a typical raw copper foil and untreated copper foil images obtained from Image J after being processed for the Matte and flat surface area. Results obtained for each copper foil are illustrated in table 3.1 & 3.2.

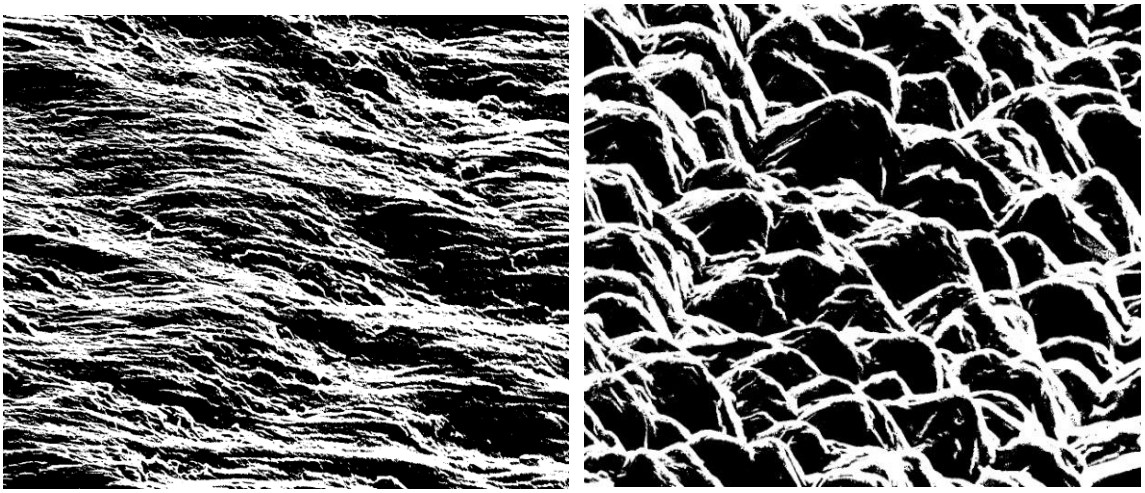

Figure 3.19 Oak-Mitsui raw copper foil (Left) & Untreated copper foil (Right)

Table 3.1 Image J Measurement for Untreated Matte Side (A_{matte}/A_{flat})

Copper Foil Type	Matte Side(A_{matte}/A_{flat})
132750C TOB III	1.23
179045B TOB III	1.625
157017A TOB III	1.324
157379A TOB III	1.009

Table 3.2 Image J Measurement for Untreated Drum Side (A_{matte}/A_{flat})

Copper Foil Type	Drum Side(A_{matte}/A_{flat})
132772C MLS	1.50
133069C MLS	2.05
133905C MLS	1.79

3.4.2 MECHANICAL PROFILER METHOD

The mechanical profiler method as previously used basically prints out a receipt of scaled profile of the copper foil being used and also include other roughness parameters. Figure 3.20 and Figure 3.21 illustrates the picture of the mechanical profiler and obtained printed receipt respectively.

Figure 3.20 The Profilometer/Perthometer

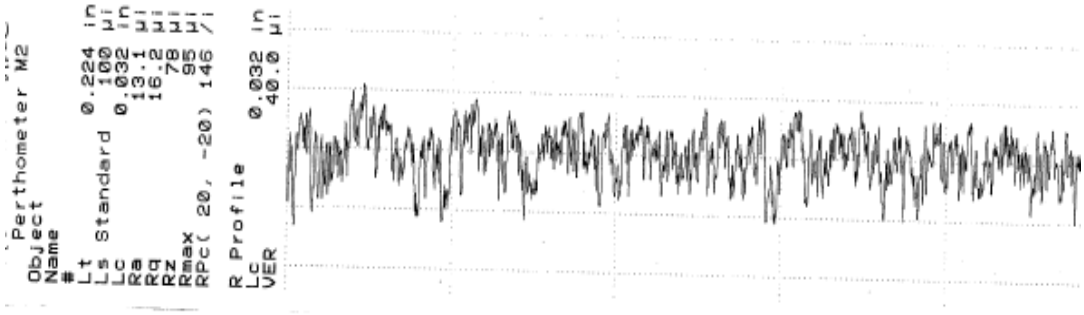

Figure 3.21 Printed receipt obtained from Perthometer

The receipts are digitally scanned and converted to discrete data points which could be further measured using the interpolation technique. This basically ensures that the length and width measurements are duly obtained

3.4.3 3D DIGITAL MICRSCOPE METHOD

For the digital microscope method, it involves taking images directly and automatically obtaining the surface area. 2D images could also be taken using JEOLJSM-

6360LV Digital microscope and imported on the 3D-KH700 HIROX microscope and measured accordingly. This basically gives a result that could be used as alternative in the absence of other methods of obtaining the required data.

CHAPTER 4

SIMULATED TOOLS: INVOLVING THE REQUIRED CHARACTERIZED PARAMETERS IN DIPOLE POWER LOSS CALCULATION

It has been recommended for a distribution of snowballs in several bins to be determined which tends to take into consideration virtually all sizes of snowballs. Using specific radii sizes for each snowball could also be used but tends to summarize a bin of snowball size into single snowball size. Also, given that the untreated copper foil surface is not the same as a perfectly flat copper surface, an assumption that $A_{matte}/A_{flat} = 1$ tends to underestimate losses below few GHz. We will then obtain required radius to be further used in this research.

4.1 RADIUS OF COPPER NODULES

Obtaining the single radius of each copper snowballs is most important for use in simulation tools available commercially. The emphasis is also placed on obtaining more accurate radii sizes of each copper snowballs as this has great effect on surface power loss results.

Previous research work[Michael Griesi-Charaterization of electrodeposited copper foil] has been able to provide information on obtaining a single effective radius and how this differs from obtaining the average snowball size. It was also clearly stated of different radii's available, which includes absolute average radius, effective snowball and average bin radius. In this research, total number of snowballs summed up to over 6x times the initial number of snowballs obtained in the previous research. The radial sizes of all snowballs

was categorized in 10bins which helps to highlight a wide distribution of the snowballs and the result of each radii snowball sizes on surface power loss. About 10 uniform snowball sizes was used so different copper foil types used could be effectively compared. This selection of snowball sizes could be used generally and it was based on result obtained after several iterations of measurements for different copper foils and types but it does not capture all the snowball sizes found on each different copper foil.

The snowball size distribution used were summarized based on a large number of bins and the selected snowball sizes was between 0.05um to 2um widely spaced in 10 bins and they were of the same snowball size distribution to effectively compare each of the copper foil performance. Some approximations were made to the snowball sizes to effectively make the snowball count for each snowball size, fit into a particular bin size for all copper foils considered.

Table 4.1 & 4.2 shows the obtained snowball distribution and the characterization of both the Matte and drum side of different copper foils considered.

Table 4.1 Characterization of snowballs (Matte Side)

					Characterization of Snowballs(Copper Nodules)(Matte Side-TOB III)									
Type	Copper Foil Name	Magnification	Angle	Total Number of Snowballs	0.05um	0.09um	0.1um	0.17um	0.2um	0.35um	0.40um	0.50um	1.0um	2.0um
1	132750C TOB III	3500X	70	6927	3960	1199	986.15	342	246	80.5	61.5	39.5	9.89	2.46
2	157017A TOB III	3500X	70	8055	4850	1405	1018.15	342	246	80.5	61.5	39.5	9.89	2.46
3	157379A TOB III	3500X	70	7339	4784.02	1111.6	799	276	199	65	58.3	36.1	7.99	1.99
4	179045B TOB III	3500X	70	7187	4750	1006.22	799	276	199	65	49.9	31.9	7.99	1.99

Table 4.2 Characterization of snowballs (Drum Side)

					Characterization of Snowballs(Copper Nodules)(Drum side-MLS)									
Type	Copper Foil Name	Magnification	Angle	Total Number of Snowballs	0.05um	0.09um	0.1um	0.17um	0.2um	0.35um	0.40um	0.50um	1.0um	2.0um
1	133905C MLS	3500X	70	2888	1090	881	374.73	245	139	63.5	49.2	34.7	8.7	2.17
2	132772C MLS	3500X	70	6786	3794	1220.13	990	341	247	80.5	61.5	39.5	9.9	2.47
3	133069C MLS	3500X	70	6713	4310	950.22	799	276	221	65	49.9	31.9	7.99	1.99
4	132851C MLS	3500X	70	6819	4052	1078	933.06	330	238	78	59.9	38.1	9.55	2.39

4.2 EXPERIMENTAL RESULTS

To obtain this required radius for the analysis, Image J was appropriately tuned and essential settings were done. The appropriate threshold was performed and scaling was done accordingly which converts the image format dimension to um. The values used were automatically generated and the mean radius was used for the snowball sizes. Figure 4.1 shows a typical imported SEM and the processed SEM.

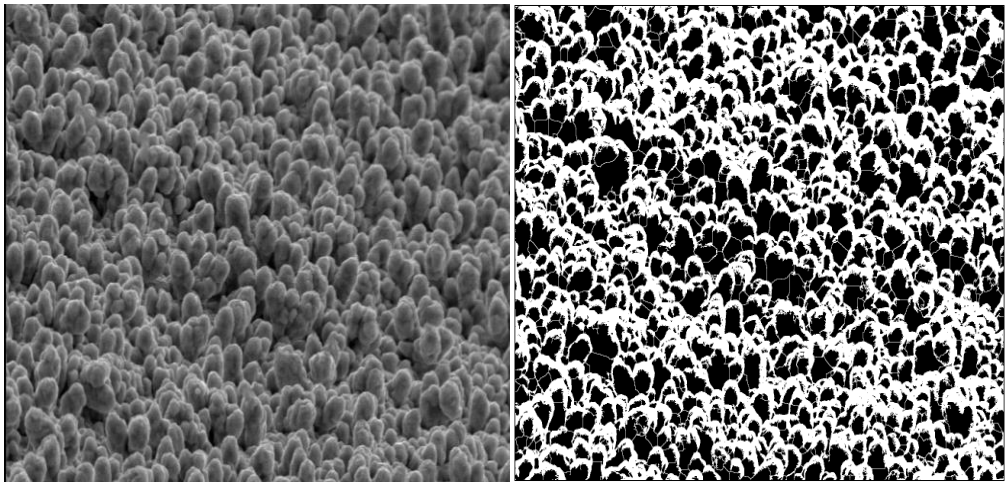

Figure 4.1 Typical Imported SEM(on the left) and Processed SEM (on the right)

There are several irregularities with regards to the manner in which the surface area for each raw copper foil are obtained using Image J. The scale used to obtain the surface area for each copper foil was 1.3E6pixels/1um.2 samples of each raw copper foil, both the (matte/drum & the flat side) were taken and tried out several times and both returned different surface area results for the flat & the matte side of the copper foil which means, the accuracy of the surface area to be obtained is not certain and also dependent on the each copper foil being obtained with respect to the same procedures to ensure consistencies and also several human errors would also play a role on how accurate the obtained result would be.

To effectively compare each copper foil, it is required to obtain the same copper foil which has the same length and width accurately, and also the SEMs being taken in the same angles.

However, different portion of the same copper foil were also taken and analyzed but turned out it might be difficult to obtain the same values for both the number of snowballs and the surface area as this varies with every portion of the copper foil taken.

Going by the obtained results, the MLS (Drum side) copper foils has higher A_{matte}/A_{flat} compared to the other ones for TOB (Matte Side) which was as a result of irregularities experienced using Image J because it is well known that, the matte side always have a higher A_{matte}/A_{flat} compared to the Drum side. This values were then further used to obtain the surface power loss of each copper foils and also showing how they differ in performance. The result of each copper foil is stated below.

4.3 Matte Side

4.3.1 TYPE132750C TOB III

The A_{matte} obtained was 1.52E-10 and the A_{flat} was 1.24E-10 which further states the ratio of the A_{matte}/A_{flat} =1.23 which indicates the roughness of the raw copper foil. The snowball sizes were distributed in 10bins from 0.05um to 2um. Figure 4.2, 4.3& 4.4 shows the result of this specific foil.

Figure 4.2 shows the dipole snowball surface power loss which involves the combination of absorption and scattering parameters. Comparing this specific copper foil with the three other foils considered on the matte side, it has losses of a little bit over 2.50 at frequency of 1THz. Figure 4.3 & 4.4 show details of the impact of the absorption and scattering properties in the surface power loss. Scattering properties tend to have

more effect when the frequency exceeds 1THz.

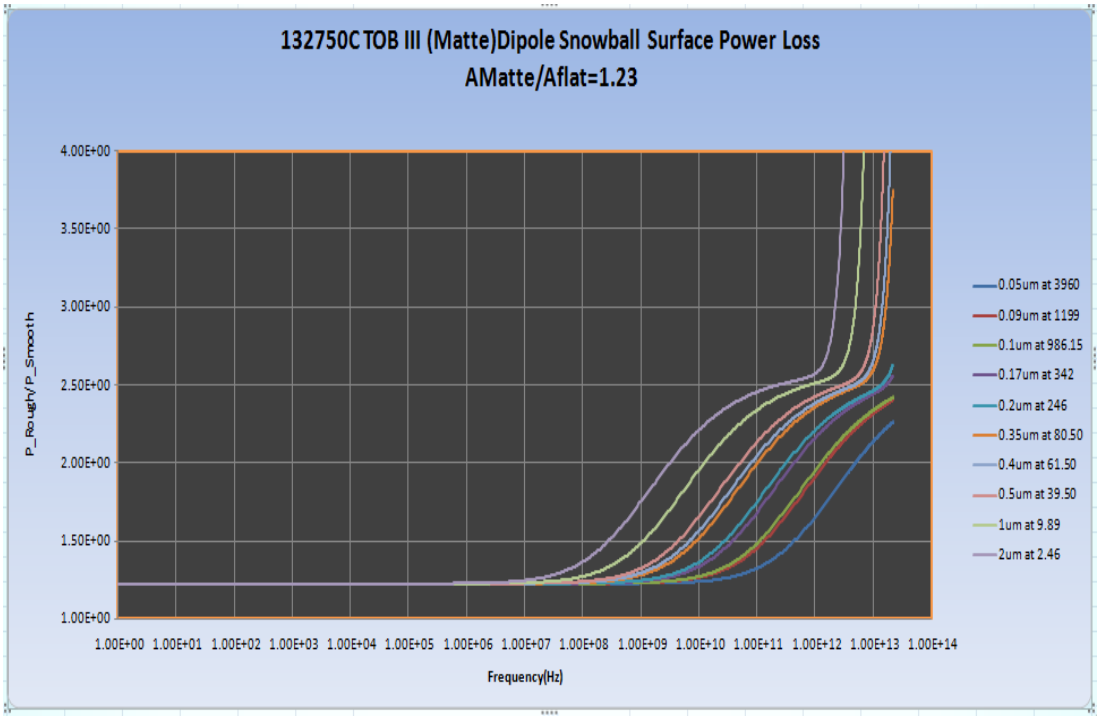

Figure 4.2 132750C Dipole Snowball Surface Power Loss

Figure 4.2 showing the combination of absorption and scattering parameters. It shows a result which extends to 1THz and how the increase in the snowball radial sizes tend to cause an increase in the surface power loss.

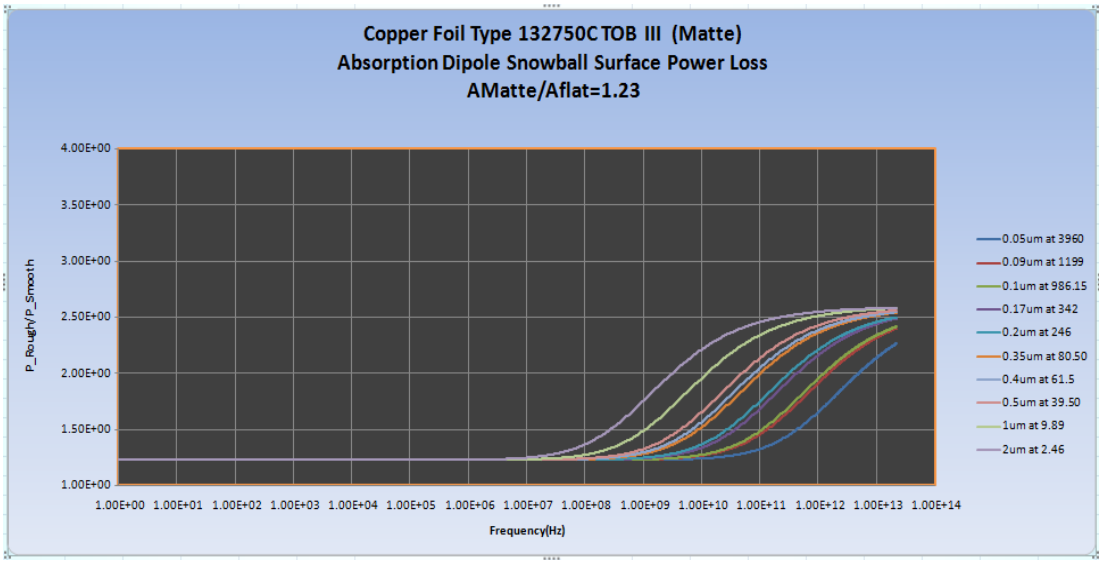

Figure 4.3 132750C Dipole Snowball Surface Power Loss due to absorption

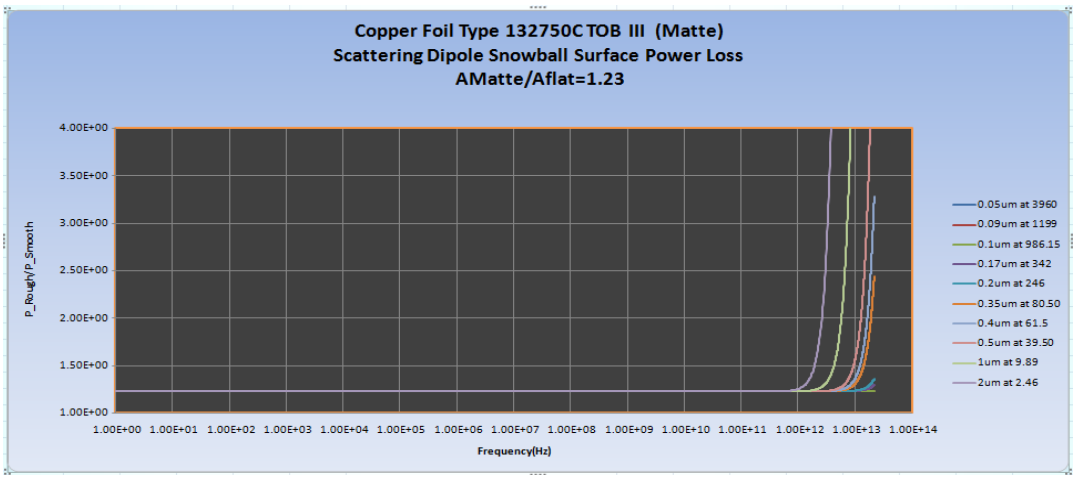

Figure 4.4132750C Dipole Snowball Surface Power Loss due to scattering

4.3.2 TYPE 179045B TOB III

The A_{matte} obtained was 1.625E-10 and the A_{flat} was 1.0E-10 which further states the ratio of the A_{matte}/A_{flat} =1.625 which indicates a higher roughness of the raw copper foil compared to the previously considered foil. The snowball sizes were distributed in 10bins from 0.05um to 2um. Figure 4.5,4.6,& 4.7 shows the result of this specific foil. Figure 4.6 & 4.7 also shows the detailed analysis of the impact of absorption and scattering parameters.

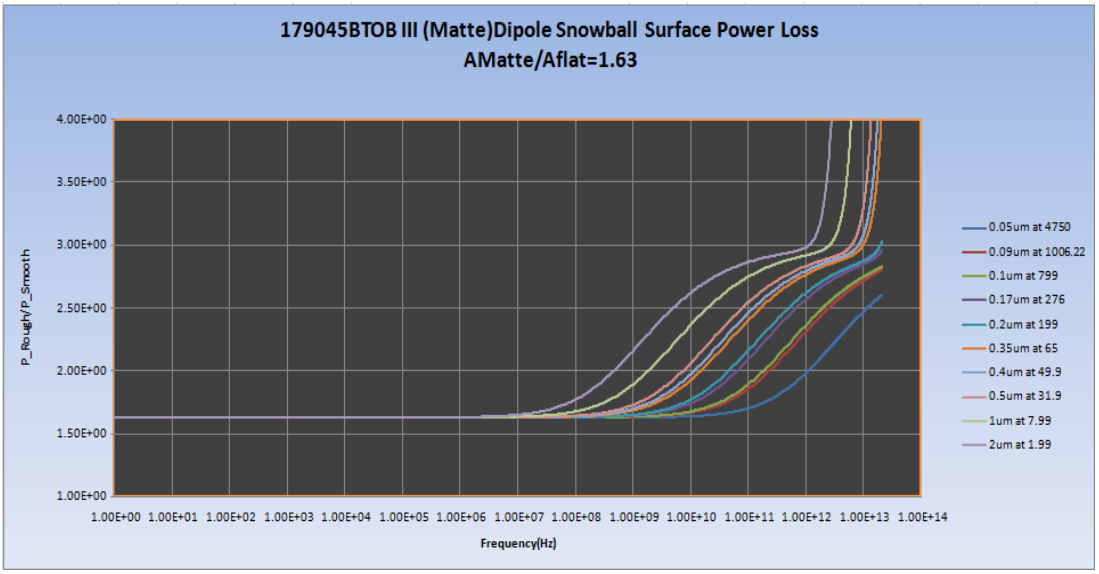

Figure 4.5 179045B Dipole Snowball Surface Power Loss

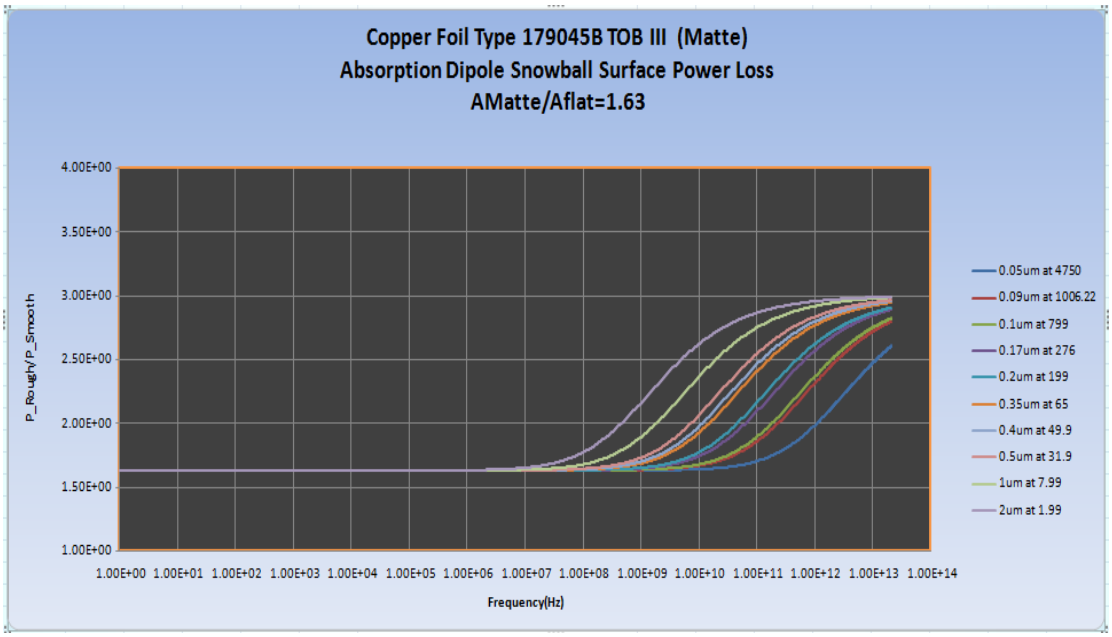

Figure 4.6179045B Dipole Snowball Surface Power Loss due to absorption

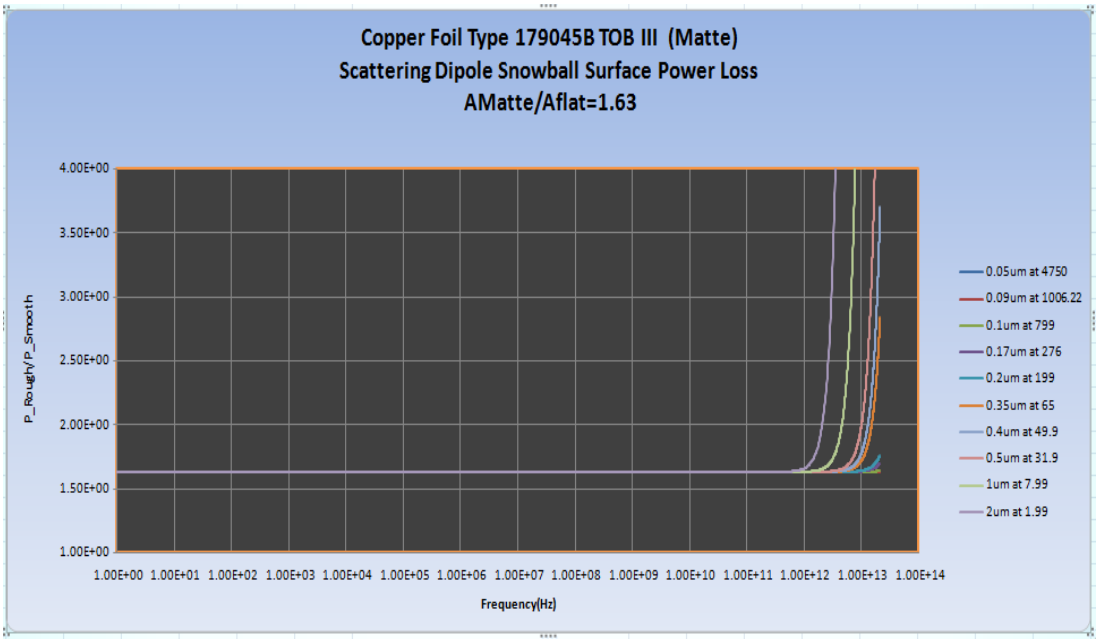

Figure 4.7 179045B Dipole Snowball Surface Power Loss due to scattering

4.3.3 TYPE 157379A TOB III

The A_{matte} obtained was 1.01E-10 and the A_{flat} was 1.0E-10 which further states the ratio of the A_{matte}/A_{flat} =1.009. The snowball sizes were distributed in 10bins from 0.05um to 2um. Figure 4.8,4.9&4.10 shows the result of this specific foil.

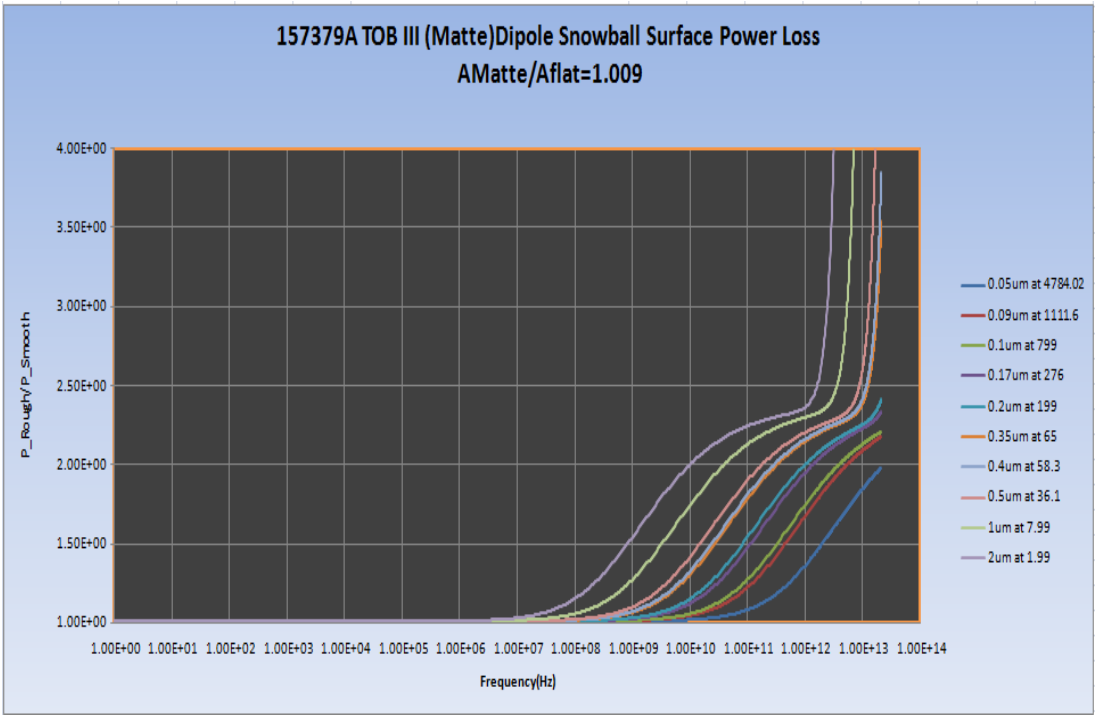

Figure 4.8 157379A Dipole Snowball Surface Power Loss

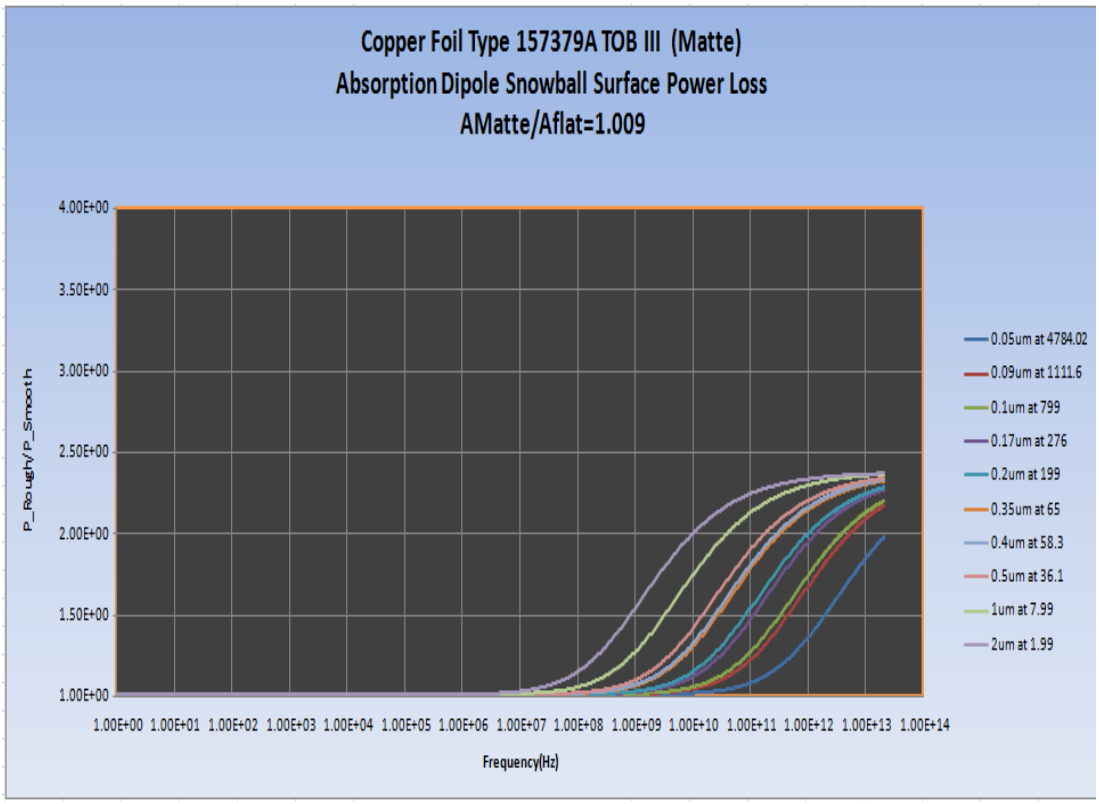

Figure 4.9 157379A Dipole Snowball Surface Power Loss due to absorption

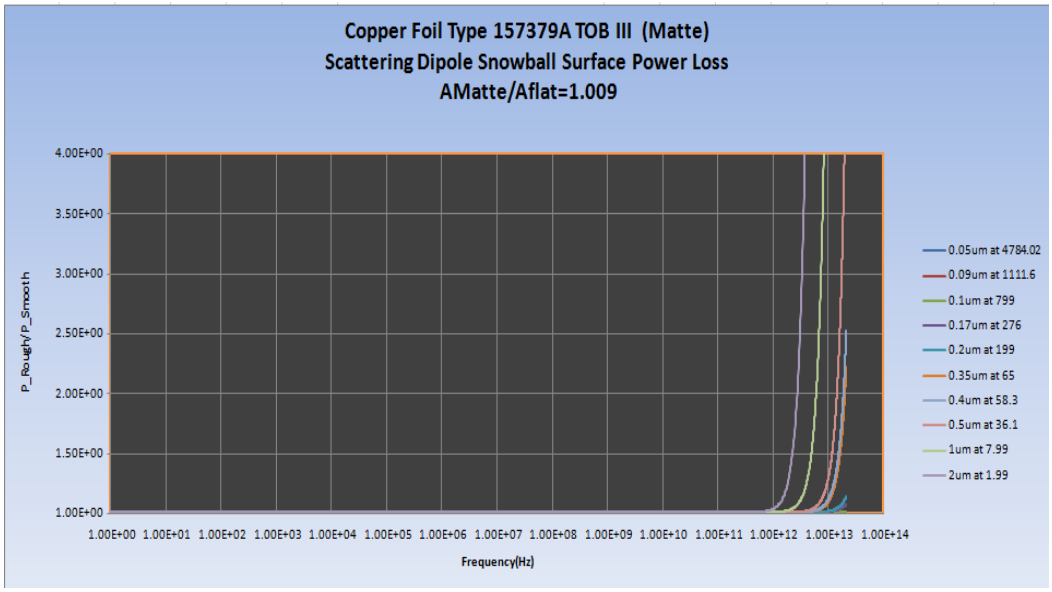

Figure 4.10 157379A Dipole Snowball Surface Power Loss due to scattering

4.3.4 TYPE 157017A TOB III

The A_{matte} obtained was 1.32E-10 and the A_{flat} was 1.0E-10 which further states the ratio of the A_{matte}/A_{flat} =1.32. The snowball sizes were distributed in 10bins from 0.05um to 2um. Figure 4.11,4.12& 4.13 shows the result of this specific foil.

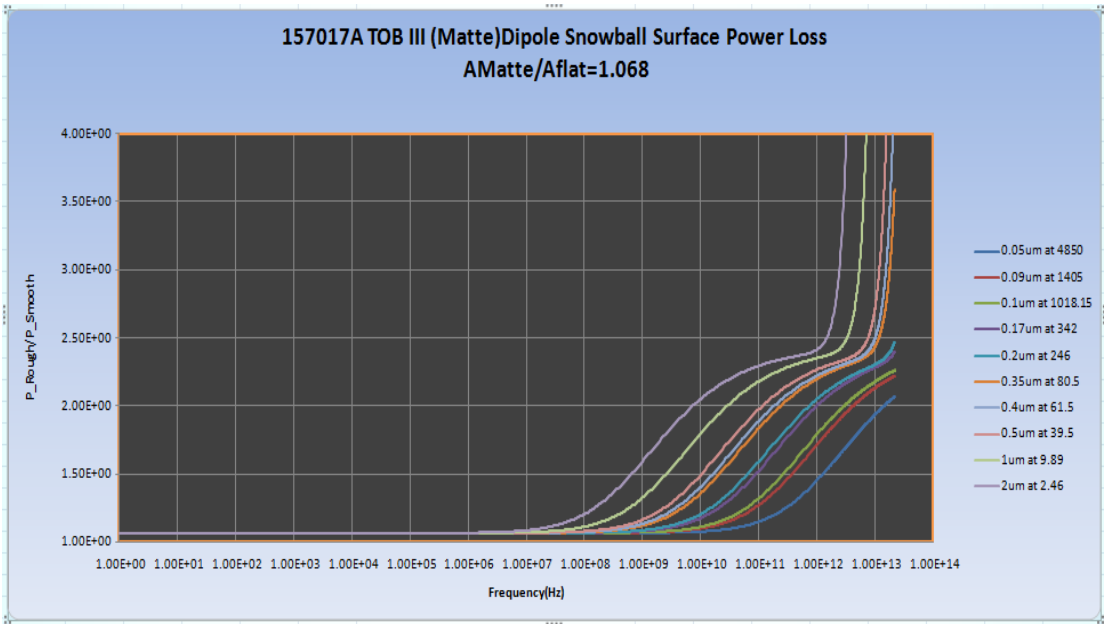

Figure 4.11 157017A Dipole Snowball Surface Power Loss

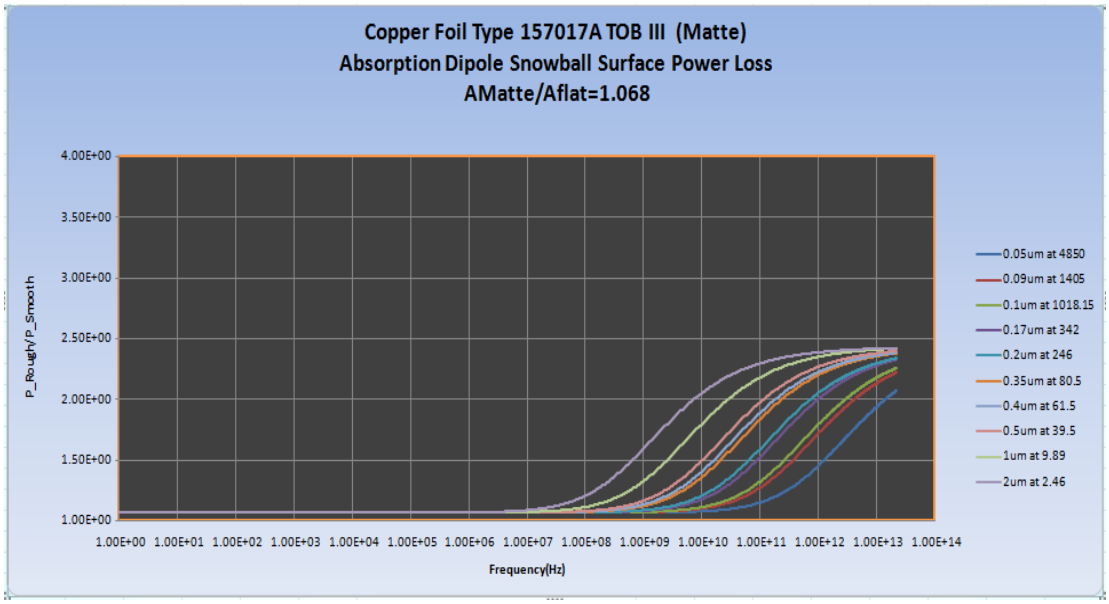

Figure 4.12 157017A Dipole Snowball Surface Power Loss due to absorption

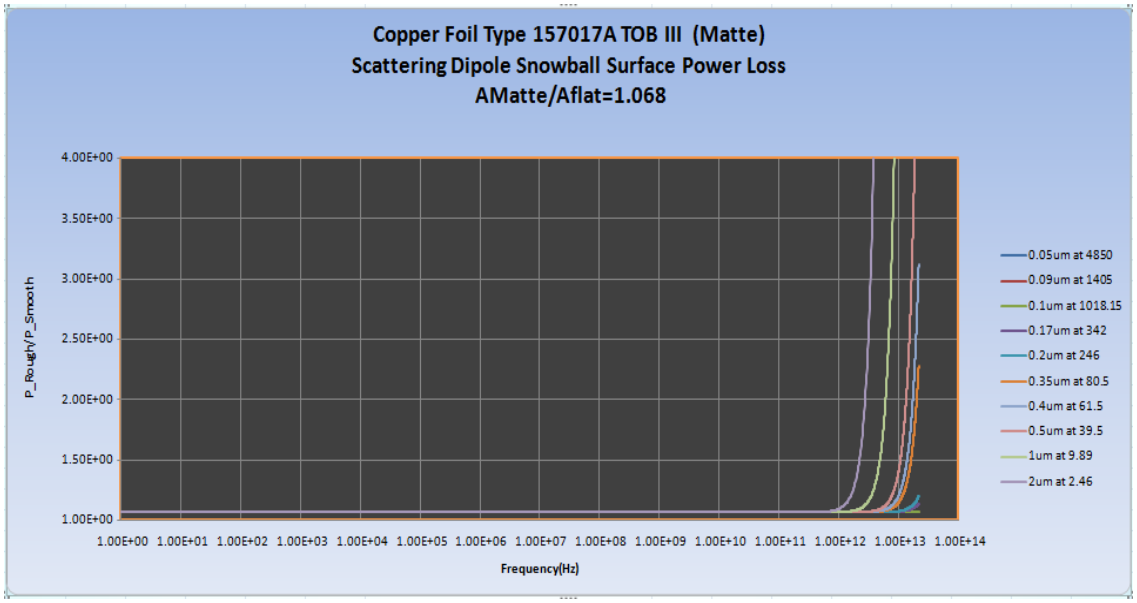

Figure 4.13 157017A Dipole Snowball Surface Power Loss due to scattering

4.4 Drum Side

The copper foils on the drum side happen to produce more losses which is due to high matte to flat surface area roughness which is in fact, been proven otherwise by the industry and also higher number of snowballs being deposited.

4.4.1 TYPE 132772 MLS

The A_{matte} obtained was 1.86E-10 and the A_{flat} was 1.24E-10 which further states the ratio of the A_{matte}/A_{flat} =1.50 . The snowball sizes were distributed in 10bins from 0.05um to 2um. Figure 4.14,4.15& 4.16 shows the result of this specific foil.

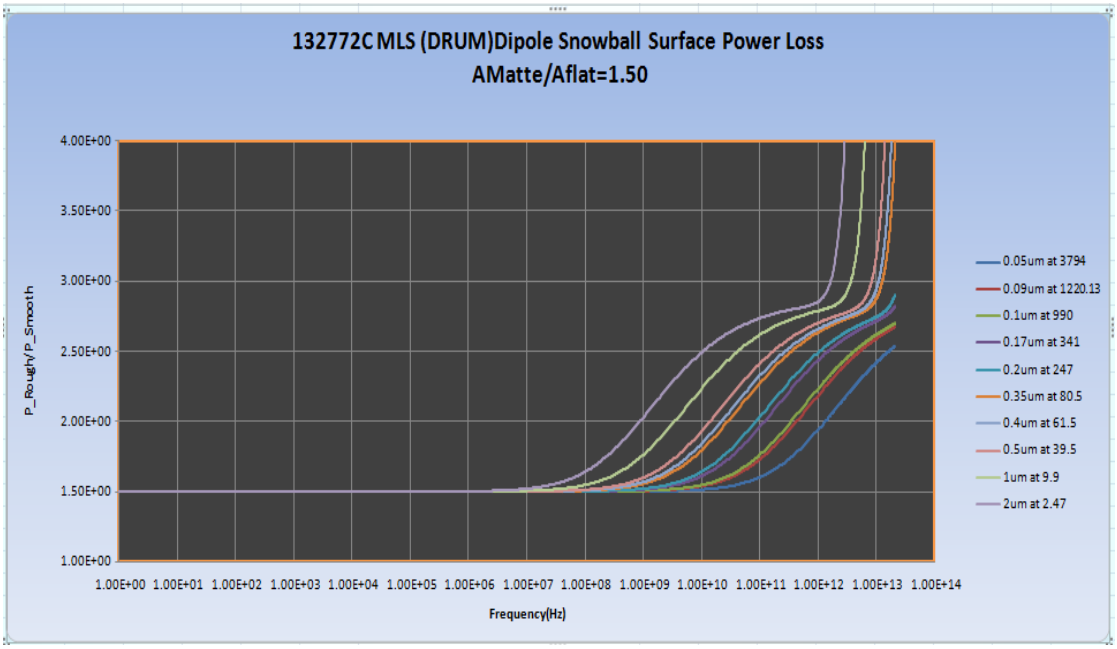

Figure 4.14 132772C MLS Dipole Snowball Surface Power Loss

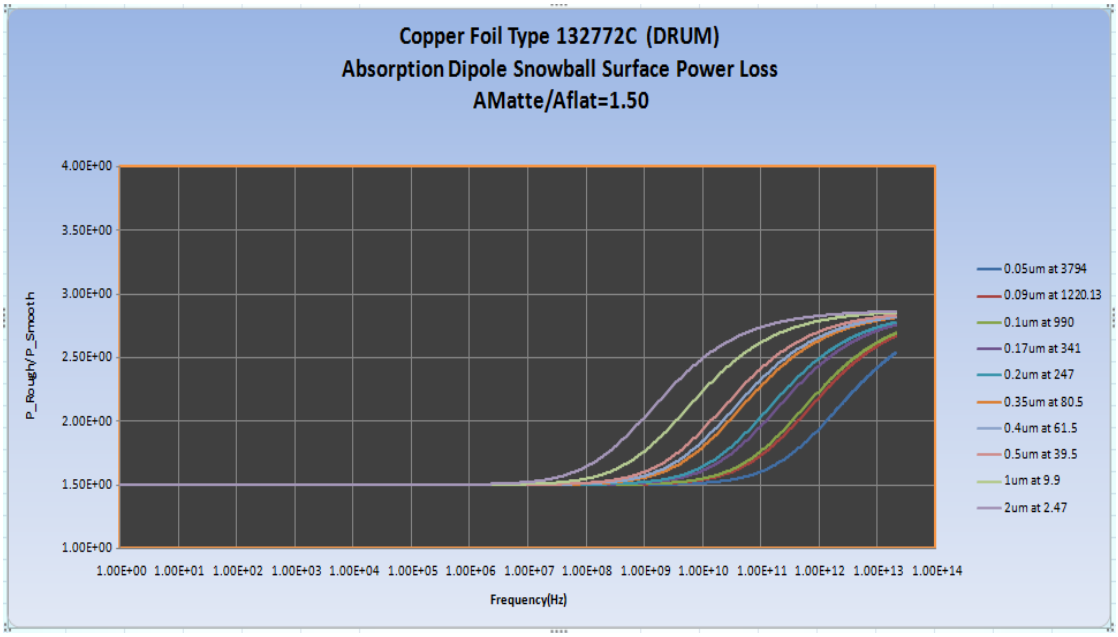

Figure 4.15 132772C MLS Dipole Snowball Surface Power Loss due to absorption

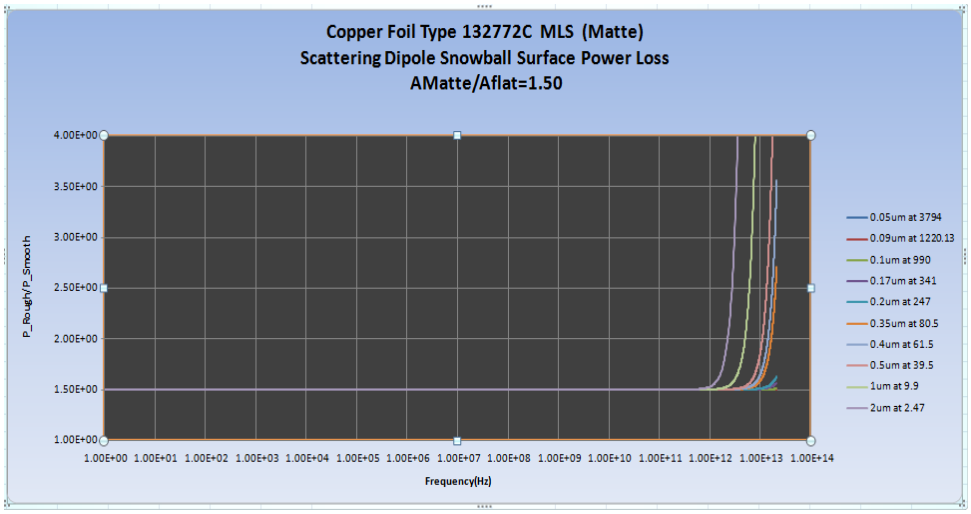

Figure 4.16 132772C MLS Dipole Snowball Surface Power Loss due to scattering

4.4.2 TYPE 133069C MLS

The A_{matte} obtained was 2.05E-10 and the A_{flat} was 1.0E-10 which further states the ratio of the $A_{matte}/A_{flat} = 2.05$. The snowball sizes were distributed in 10bins from 0.05um to 2um. Figure 4.17,4.18& 4.19 shows the result of this specific foil. The Matte to flat surface area ratio was higher than other copper foils considered both on the matte and the drum side which indicates higher surface roughness which would definitely lead to more losses.

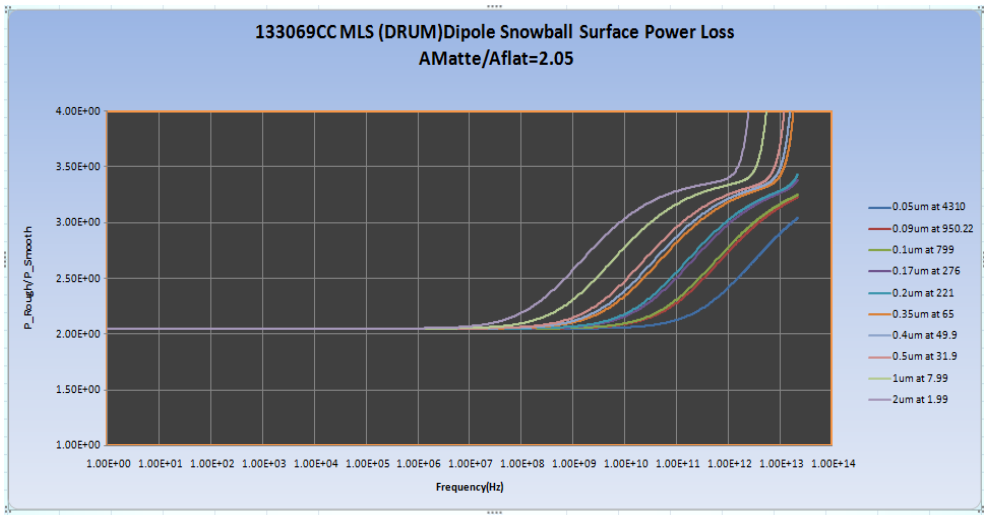

Figure 4.17 133069C MLS Dipole Snowball Surface Power Loss

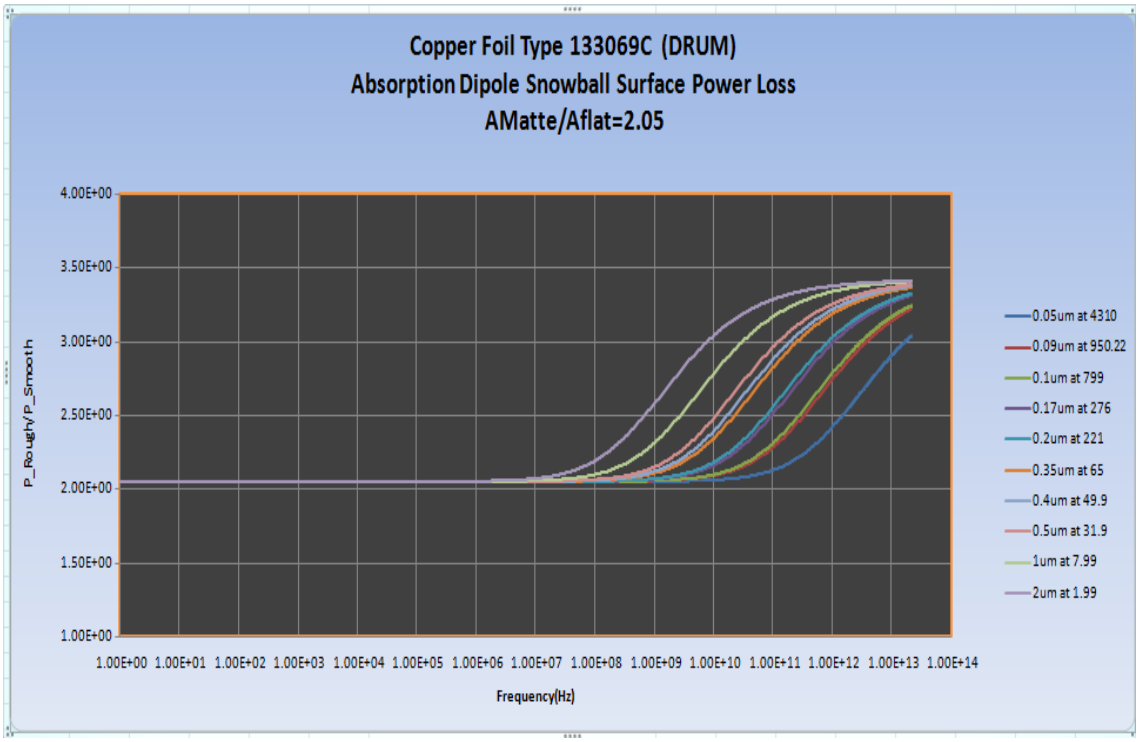

Figure 4.18 133069C MLS Dipole Snowball Surface Power Loss due to absorption

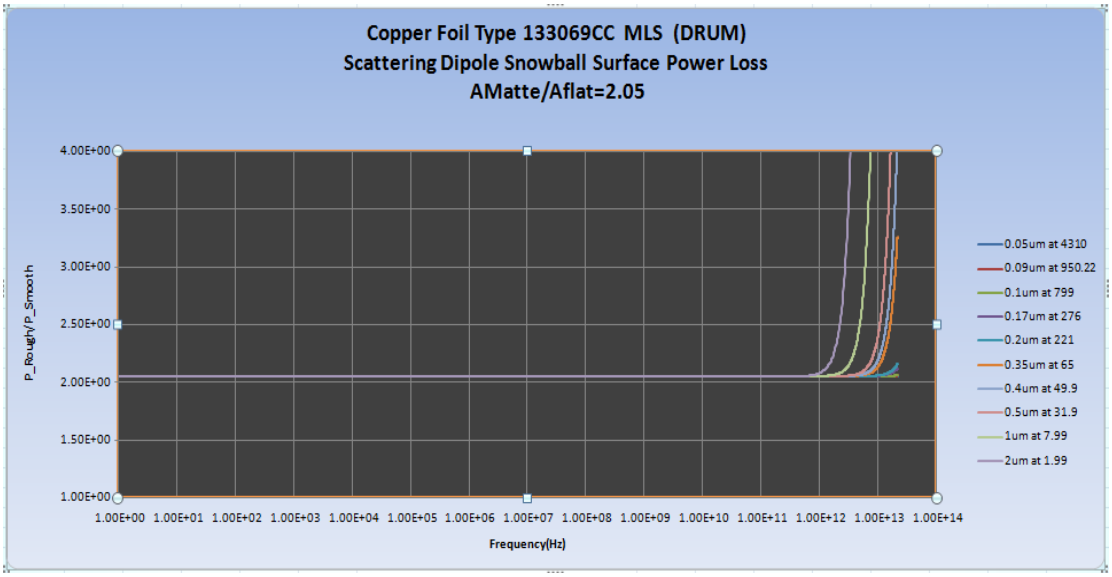

Figure 4.19 133069C MLS Dipole Snowball Surface Power Loss due to scattering

4.4.3 TYPE 133905C MLS

With the matte to flat surface area of about 1.730, it has losses which exceeds 3.0 as the frequency tends towards 1THz. Figures 4.20,4.21 & 4.22 illustrates the result of the

losses for this specific copper foil and the effect of absorption and scattering parameters.

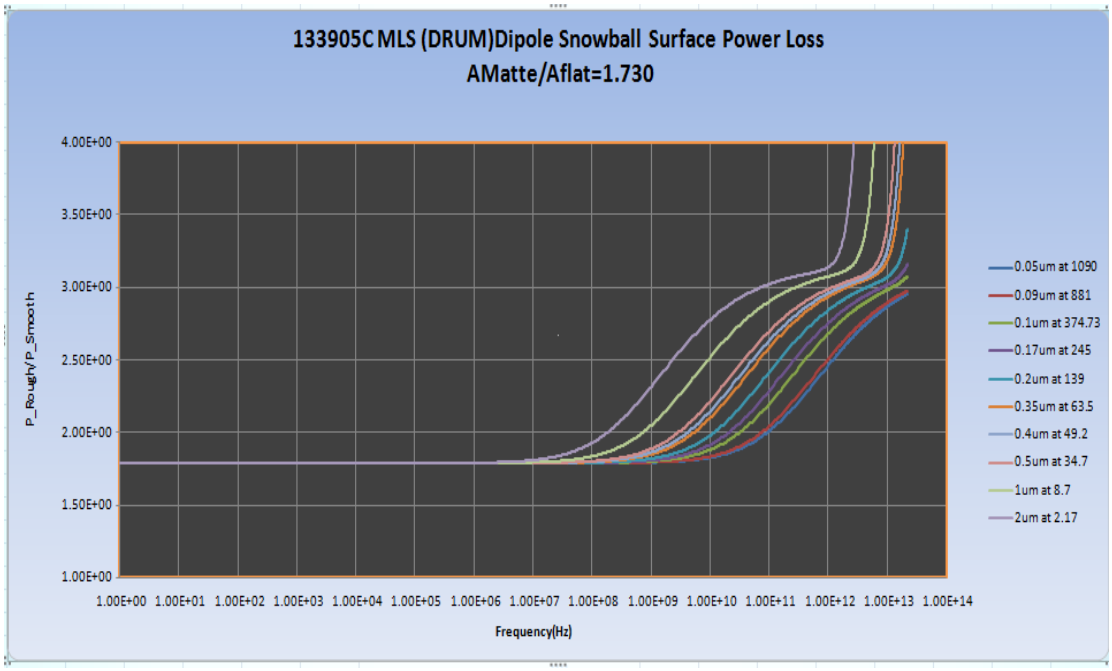

Figure 4.20 133905C MLS Dipole Snowball Surface Power Loss

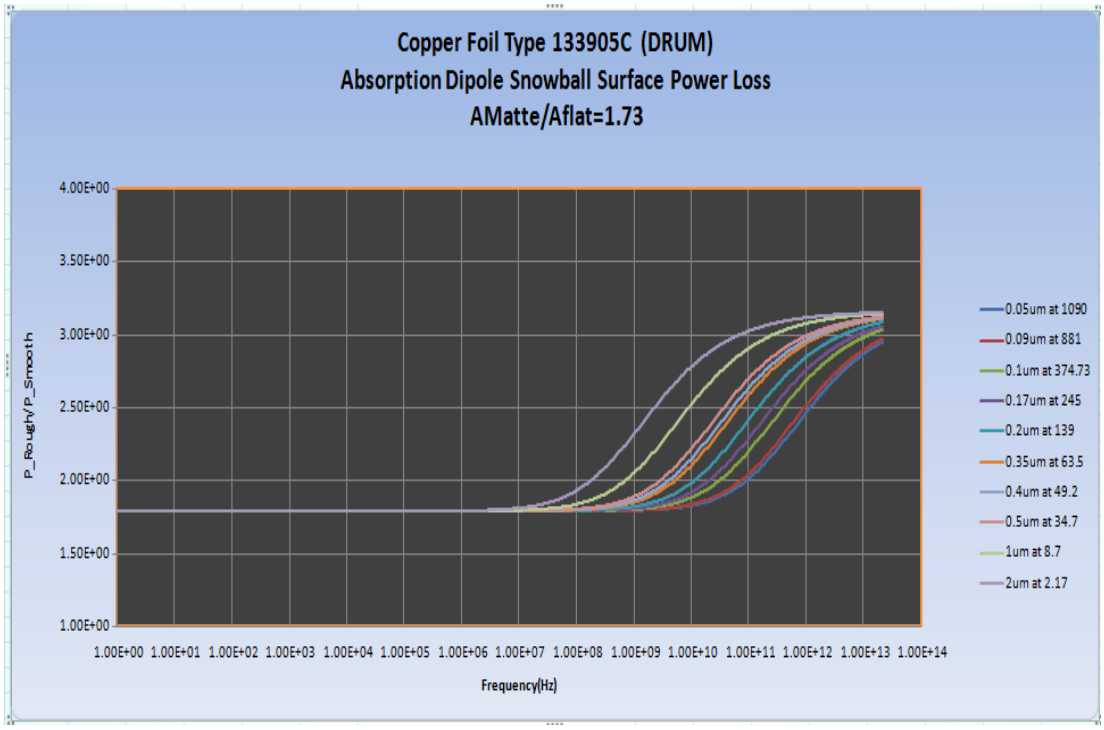

Figure 4.21 133905C MLS Dipole Snowball Surface Power Loss due to absorption

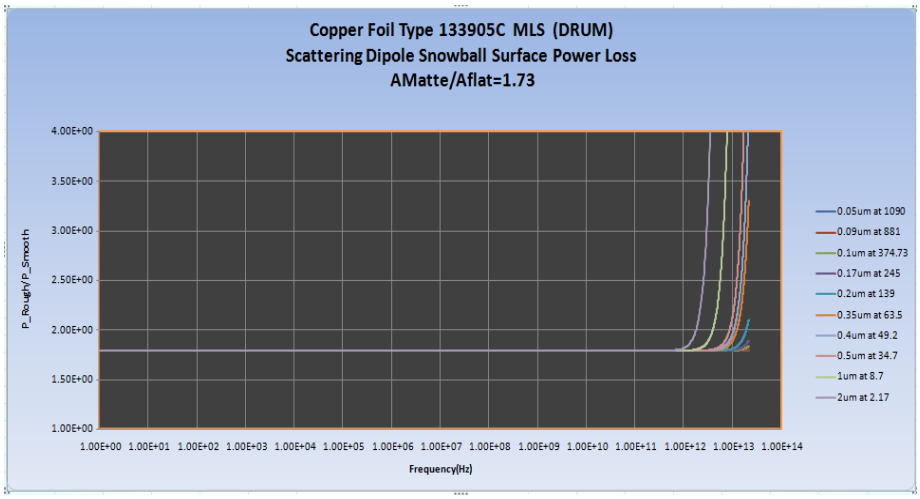

Figure 4.22 133905C MLS Dipole Snowball Surface Power Loss due to scattering

4.5 IMPACT OF N_I INCREASE ON DIPOLE SNOWBALL SURFACE POWER LOSS

To further continue with this research, a factor, N_i increase, was considered to know the impact it has on the surface power loss. A specific snowball radius was selected(a_i=1um) which was made constant and there was increase in the number of snowballs(2x,3x and 4x the initial number of snowballs). The matte to flat surface area was made constant for all increases and there was indeed more losses with respect to the increase in the number of snowballs. Figure 4.23 shows the result obtained. It should be noted that $A_{matte} = A_{flat}$, and the assumption was that A_{matte}/A_{flat}= 1.0.

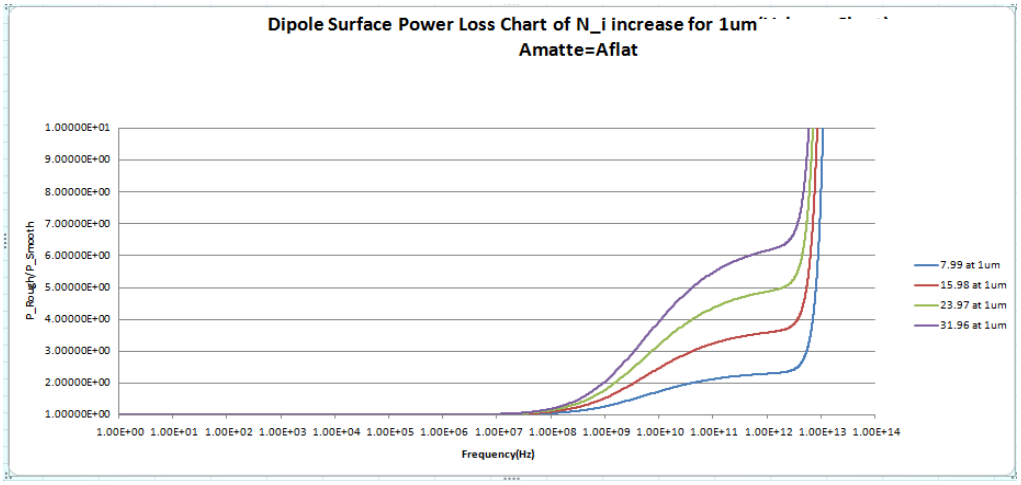

Figure 4.23 Dipole Snowball Power Loss of N_i increase for snowball radius of 1um

It is clear at this point that different copper foils have different losses which will definitely affect the performance of devices. It is also clear how it is difficult to obtain the same results for the surface area of the same copper foil because different points on a specific roll of copper foil produces different results. Also the losses due to scattering were mostly experienced beyond a frequency of 1THz which shows scattering parameters has negligible effect for frequencies below 1THz.Surface roughness of the copper foils before the snowballs were deposited, also played a major role in the losses experienced which indicates more emphasis should be placed on maintaining considerable matte to flat surface roughness to avoid unnecessary losses experienced.

4.6 IMAGE J DATA VALIDATION

To further validate Image J data, one of the copper foils (Oak-Mitsui 133905C) was selected to obtain snowball count and compare with that obtained by Image J. The Grid method was used to obtain an approximate snowball count. The Grid consists of 12 x 16 boxes and each snowball is being counted manually. In total, about 1236 snowballs were counted compared to Image J count of 2888 which means that the image J results are fairly accurate considering the fact that manually counting the snowballs has errors such as, hidden snowballs, snowballs in layers, and missing snowballs in counting.

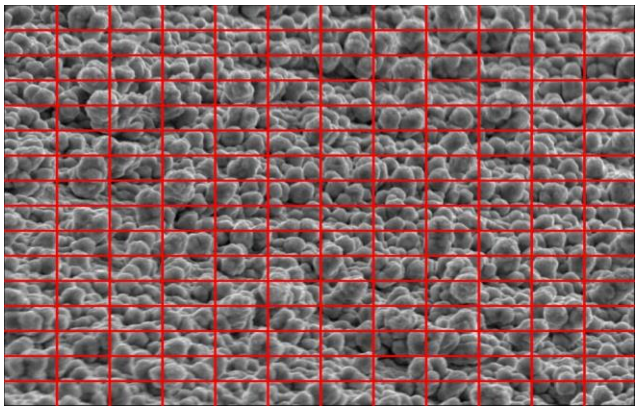

Figure 4.24 Image Grid of SEM to manually count snowballs

CHAPTER 5

ANALYSIS AND DISCUSSION

5.1 OBSERVATIONS AND CONCERNS

While the method used for this research is understandable and could be easily carried out, it is with some speculations there might still be some hidden snowballs which were not properly captured which definitely won't be revealed on the SEMs which will make it difficult for the software used to obtained such hidden snowballs. The height of the stack of snowballs is also essential to properly estimate the volume of the snowballs. Furthermore, it is really difficult to obtain accurate results considering different points on a roll of a specific copper foil which makes it difficult to obtain a standard approach to obtaining a standard surface power loss for all copper foils under consideration.

While it is well known that the Matte side has a higher surface area ratio compared to the drum side, which indicates more losses is expected on the matte side, the results obtained in this research were however due to Image J producing a larger A_{matte}/A_{flat} for the drum side compared to the matte side. This is thought to be as a result of :

1. Deviations occurring as a result of taking different samples of different copper foil type.
2. Image J also introduced some errors in which it would require unique scaling for each of the copper foil type in consideration, and using the same scale for each of the copper foil types to effectively compare each of this

copper foil type in terms of Amatte/Aflat, snowball counts, and radial sizes of the snowballs in said to introduce such errors.

3. Not having the exact same size of copper foil type sample that are placed in the SEM to obtain the SEM images.

With the assumption of $A_{matte}/A_{flat} = 1.06$ being used for all copper foils, there is indeed more losses experienced on the Matte Side compared to the drum side.

5.2 MAJOR CONTIRBUTIONS

First, an alternative method of characterization analysis has been presented. This has helped to improve the accuracy of parameters needed for the implementation of dipole snowball model which includes snowball radial size (a_i),Matte Area,(A_{matte}), Flat Surface Area (A_{flat}) and total number of snowballs(N_i).

Secondly, industry engineers will get to understand that scattering cross-section does have a significant impact above 1THz on surface power loss which has been well illustrated in this thesis which it is a significant contribution to scientific literature . This thesis has also demonstrated the impact dipole and quadrupole terms have on implementation of the snowball model.

Thirdly, this would help ED copper foil industry, especially Oak-mitsui, whose copper foils were used, to characterize copper foils based on the surface power loss. This thesis has inadvertently provided insight on the performance of some of the copper foils being manufactured.

Fourthly, this thesis has shown the impact snowball increase has on surface power loss, which would give an insight to the industry on the need for reduction in the deposition of snowballs on the ED copper foils.

In its entirety, this thesis has advanced our knowledge of high-speed conductor losses, made recommendations on how this could be reduced and will further improve high speed circuit designs.

CHAPTER 6

FUTURE WORK AND RECOMMENDATION

6.1 FUTURE WORK

This would involve including Quadrupole terms in calculations for the Huray snowball model especially for frequency beyond 1THz to ascertain that the terms are indeed negligible.

Also some work needs to be done in the area of obtaining accurate snowball radii distribution which involves creating bins of different snowball sizes, and accurately obtaining the snowball sizes. This will indeed help with accurate high speed circuit modeling with and accuracy of surface power loss prediction.

Also, performing VNA measurements using the obtained values to properly validate the measurements using Image J.

6.2 RECOMMENDATION

Based on the need to accurately characterize copper snowballs and obtain accurate radial sizes of snowballs, there is need to obtain a more accurate equipment or method, such as Optical 3D Microscope which helps to accurately count the total number of snowballs, and snowball sizes without any form of contact with the copper foil.

There is also need for copper foil manufacturing companies to reduce the number of copper nodules that is been deposited on this copper foils which has indeed proven to increase surface power loss.

REFERENCES

1. http://www.keysight.com/upload/cmc_upload/All/MicroAppsRoughness.pdf?&cc=US&lc=eng

2. S. Hall et al., "Advanced Signal Integrity for High Speed Digital Design" John Wiley & Sons, Inc., 2009, pp. 222-243

3. P. Huray, *The Foundations of Signal Integrity*. Hoboken, NJ: John Wiley & Sons, Inc., 2010, pp. 109-144, 216-276

4. P. Pathmanathan, "Power Loss due to Periodic Structures in High-Speed Packages and Printed Circuit Boards," *Microelectronics and Packaging Conference (EMPC), 2011 18th European*, 12-15 Sept. 2011, pp.1-8

5. M. Griesi *et al.*, "Electrodeposited Copper Foil Surface Characterization for Accurate Conductor Loss Modeling," *Design Con 2015*, 2015

6. Michael Griesi, "Characterization of Electrodeposited Copper Foil Surface Roughness for accurate Conductor Power Loss Modeling," MS Thesis, Dept. of Elec. Eng., Univ. of South Carolina, Columbia, SC 2014

7. Image J [Online] Available: https://imagej.nih.gov/ij/docs/guide/user-guide.pdf

8. Image J [Online] Available: https://imagej.nih.gov/ij/docs/pdfs/examples.pdf

9. Image J [Online] Available: https://imagej.nih.gov/ij/docs/pdfs/Image_Processing_with_ImageJ.pdf

10. Tektonix., "Fundamentals of Signal Integrity" 2007, pp. 9 – 24

11. C. Balanis, *Advanced Engineering Electromagnetics*. Hoboken, NJ: John Wiley & Sons, Inc., 2012, pp. 655-664

12. https://www.plda.com/market-ready-conquer-pcie-40-challenges